R. & M. No. 3670

R. & M. No. 3670

MINISTRY OF DEFENCE

AERONAUTICAL RESEARCH COUNCIL
REPORTS AND MEMORANDA

A Simulation of the Low Speed Handling of the BAC 221 Slender-Wing Research Aircraft

By T. WILCOCK

Aero Flight, R.A.E., Bedford

LONDON: HER MAJESTY'S STATIONERY OFFICE
1971
PRICE £1·65 NET

A Simulation of the Low Speed Handling of the BAC 221 Slender-Wing Research Aircraft

By T. WILCOCK

Aero Flight, R.A.E., Bedford

Reports and Memoranda No. 3670*
November, 1969

Summary.

A piloted flight simulator study of the low speed handling of the BAC 221 slender-wing research aircraft was performed for validation of the simulation of slender-wing supersonic transport aircraft. The lateral representation of the aircraft was satisfactory, and lateral control problems experienced on the real aircraft at high angles of incidence were reproduced on the simulator and investigated in more detail than would be practicable in flight. There were several discrepancies in the longitudinal characteristics of the simulation, some of which can be attributed to inadequate representation of visual cues: satisfactory explanation of other discrepancies has not yet been obtained but a further simulation may resolve these problems. Sidestep manoeuvres and crosswind landings were studied, and the overall quality of the simulation is discussed in relation to previous supersonic transport aircraft simulations.

CONTENTS

1. Introduction

2. Description of Aircraft and Simulator

   2.1. The aircraft

   2.2. The simulator

3. Tests Made

4. Flight-Simulator Comparison

   4.1. Longitudinal comparison

   4.2. Lateral comparison

   4.3. Simulation of touchdown

*Replaces R.A.E. Tech. Report No. 69257—A.R.C. 32 262.

5. Sidestep Manoeuvres

6. Crosswind Landings

7. Lateral Control Problems in High Incidence Flight

8. Discussion and Simulator Validation

   8.1. Representation of the BAC 221

   8.2. Relevance to previous SST simulation

9. Conclusions

List of Symbols

References

Appendix Aircraft data as used in the simulation

Illustrations—Figs. 1 to 26

Detachable Abstract Cards

1. *Introduction.*

One of the problems facing the operators of flight simulators used for pre-flight research into new aircraft is that of validation of the simulator, particularly when the aircraft simulated has unconventional features. Some measure of confidence in the simulator results can be obtained by a comparative simulation of an aircraft already in use and of the same category as, or possessing similar handling features to, the new aircraft under investigation.

The Aero Flight research simulator at R.A.E. Bedford has been used recently for extensive studies of the handling of a slender-wing supersonic transport aircraft (SST)[1,2] during take-off and landing, and validation of the results was required. For this purpose a simulation of the BAC 221 slender-wing research aircraft was prepared.

The BAC 221[3] is a single seat aircraft with a flight envelope extending from low to supersonic speeds. Although not of comparable size to the simulated SST (which was based on the prototype Concorde design at December 1965), it possesses many of the aerodynamic features of that aircraft. Also it is operated by R.A.E. Bedford and some of the R.A.E. pilots involved in the SST simulations had flown it.

The simulation was prepared from wind tunnel data[4,5] (no detailed flight measurements of aerodynamic derivatives were available) and the behaviour over the speed range 100–200 kt eas was simulated in some detail. The general handling of the simulated aircraft during take-off, approach and landing was assessed by the pilots for comparison with the real aircraft, and particular studies of crosswind approaches and landings and sidestep manoeuvres on the approach were performed. The opportunity was also taken to investigate in further detail some control problems encountered in flight at high incidence. Finally, recovery from speeds below the zero rate of climb speed[6] was investigated; this topic will be discussed in a separate report[7].

The particular aerodynamic features of the BAC 221 and the possible relevance to Concorde have been discussed by Barnes[3] but a few points are worth extra mention here. In particular the inertia distribution of the aircraft (low roll inertia, high pitch and yaw inertias) imposes a constraint on the motion of the aircraft such that the Dutch roll mode and the response to aileron are almost confined to a pure rolling motion about the principal roll inertia axis, particularly at low speeds. At low speed the incidence angle is large (14° at 150 kt, 20° at 120 kt) and, in rolling about the principal inertia axis, some of this incidence is converted into sideslip. The rolling moment due to sideslip derivative l_v is large and negative and the damping in roll is low; all these features combine to give a potentially oscillatory roll behaviour, and the large $-l_v$ and low roll damping suggest a considerable response to lateral gusts. A further feature affecting lateral handling is that of appreciable adverse yaw from the outboard ailerons at high incidence, leading to problems of yaw divergence while controlling bank angle. In the longitudinal plane, the low aspect ratio leads to a high minimum drag speed, and approaches are made under conditions of negative speed stability.

Thirty four sessions, totalling 27 hours, were flown by the four Aero Flight test pilots during the simulation; two of these pilots had flight experience of the aircraft. In addition a third pilot familiar with the aircraft, and previously with Aero Flight, performed one session of $1\frac{1}{2}$ hours. The simulation took place at the end of 1967.

2. *Description of Aircraft and Simulator.*

2.1. *The Aircraft.*

The BAC 221 is a single seat, single engined research aircraft built to investigate the flight characteristics of a slender-wing design[3]. The aircraft wing is of ogee shape and has an aspect ratio of 1·28 and a minimum leading edge sweep of 65°. Fig. 1 is a general arrangement of the aircraft in the clean configuration and Fig. 2 shows the aircraft in the approach configuration. As shown in the photograph, the nose of the aircraft, including the cockpit, is hinged and is lowered 8° for approach and landing to improve the pilot's view.

Control of the aircraft is by separate elevators, ailerons and rudder, the elevators being mounted inboard and the ailerons outboard on the wing trailing edge. Control stick to surface sensitivity of ele-

vators and ailerons is continuously variable over the range 1:1 to 9:1 for elevators and 1:1 to 6:1 for ailerons*. An interconnection between aileron and rudder which gives a rudder angle proportional to, and in phase with, the pilot's applied aileron angle can be selected if required.

Data on the aircraft and control systems are given in the Appendix.

2.2. *The Simulator.*

The simulator consists of a single seat cockpit mounted on a motion system and using a closed-circuit television visual display[8]. Fig. 3 shows the cockpit and motion system and Fig. 4 the pilot's view of the instrument panel and visual display. Cockpit motion was provided in pitch and roll, the displacements of the cockpit being directly proportional to the aircraft's computed pitch and roll attitudes (the proportionality being 50 per cent for pitch and 38 per cent for roll). The pilot sat some six feet ahead of the pitching pivot and so experienced some incidental vertical motion coupled with the pitch motion, but this was unrepresentative of the true vertical motion of the aircraft cockpit.

The pilot's 'outside world' view was provided by a closed-circuit television system in which a television camera views a scale model (1:2000) of an airfield and surrounding countryside. Motion of the camera relative to the model is controlled by the simulator computer in response to the computed position and angular orientation of the aircraft, and the picture so produced is projected onto a screen outside the simulator cockpit, six feet in front of the pilot. The angular field of view provided by the display is 45° in azimuth and 35° in pitch; the sides of the cockpit hood were blacked out to restrict the pilot's view to the projector screen.

The pilot's controls consisted of a conventional stick and rudder pedals, a throttle lever mounted on the left-hand console, switches for the control of simulated undercarriage and nose droop operation, and control gearing selectors. Gearings were not fully variable as in the aircraft but were limited to the fixed ratios of 1:1, 1·5:1 and 2:1 for the elevators and 1:1, 2:1 and 4:1 for the ailerons. However, gearings outside these ranges are not used in the aircraft for the speed range simulated. Elevator trim was provided by a thumb-operated switch on the control column. Trim of aileron and rudder were not available, unlike the real aircraft.

The simulator flight instruments are shown in Fig. 4 and comprise:-

Top row: incidence, sideslip, normal acceleration
Middle row: airspeed, artificial horizon, vertical speed, engine rev/min
Bottom row: radio altimeter, pressure altimeter, compass, turn and slip, ILS, elevator trim position.

The instruments used were similar to those in the real aircraft, though their layout was not accurately represented. The aircraft did not have an ILS meter or radio altimeter.

Aural cues consisted of simulated engine noise and of wheel rumble when the aircraft was running along the ground.

Continuous solution on an analogue computer of the equations of motion for a rigid aircraft determined the simulated aircraft's behaviour in response to control inputs and external disturbances. The aerodynamic characteristics of the simulated aircraft were based on wind tunnel and theoretical data[4,5] and are summarised in the Appendix. The computation included variations in the aerodynamics due to ground proximity and also a simplified representation of undercarriage behaviour. Atmospheric disturbances in the form of steady winds or turbulence could be introduced.

Ref. 4 was the primary source of static aerodynamic data, with the exception of the yawing moment due to sideslip n_v in the clean configuration, for which some unpublished R.A.E. wind tunnel results[5] were used, Ref. 4 giving insufficient coverage at high incidence. The value of n_v in these results differed from that in Ref. 4 and as a result the stability roots quoted in section 7 differ from those used in previous work based on the Ref. 4 value of n_v. Confirmation of the value of n_v from flight tests has not been possible as the aircraft's flight programme has included little time for derivative measurements. In any case, the difficulty of maintaining steady conditions at high incidence hinders any attempt to measure derivatives.

*A gearing of 9:1 means that full stick movement gives 1/9 of full control surface travel.

3. *Tests Made.*

Thirty-four simulation sessions, totalling 27 hours, were flown by the four Aero Flight test pilots. An ex-Aero Flight pilot also flew one session of $1\frac{1}{2}$ hours; this pilot and two of the others had a combined total of around 30 hours of flight in the actual aircraft. The remaining two pilots had not flown the BAC 221 but have since done so.

Most of the tests were made in the approach configuration and studied handling during the approach and landing phases of flight. The general handling was assessed by the pilots for comparison with the real aircraft, and particular studies of sidestep manoeuvres and crosswind landings were performed. The lateral behaviour at high incidence in the clean configuration was examined in some detail, but it was necessary to perform the tests under instrument flight conditions as the visual display was unsuitable for this flight regime.

Section 4 considers the validation of the simulation, sections 5 and 6 discuss sidesteps and crosswind landings respectively, and section 7 is concerned with the behaviour at high incidence.

4. *Flight-Simulator Comparison.*

Measurements in flight of the stability characteristics of the BAC 221 are few and are limited to high altitude conditions[3,9]. The simulator tests were performed at sea level conditions and thus quantitative evaluation of the data used in the simulation is not possible. Assessment of the accuracy of the simulation is therefore limited to pilots' comments and to records of similar manoeuvres in aircraft and simulator.

Three pilots who took part in this simulation had flown the aircraft for a combined total of around 30 hours. However, the aircraft had not flown during the nine months prior to the simulation nor did it fly in the following six months, so subjective impressions of the realism of the simulator were limited by lack of recent experience in the aircraft.

Comparison of the aircraft and simulator will, for convenience, be divided into separate descriptions of the longitudinal and lateral handling features, with a third sub-section on the behaviour during touchdown. Sections 5, 6 and 7, which consider particular flight conditions also contain some flight-simulator comparisons.

4.1. *Longitudinal comparison.*

Criticisms of the simulator as initially set up were that the elevator was too sensitive, there was a marked trim change with power whereas none was present in the aircraft, and that the strong simulated nose-down pitching moment due to ground effect was not characteristic of the real aircraft. Pitching moment from thrust was included initially since the engine thrust line does not pass through the c.g, but as no pitching moment was evident in flight it was thought that intake momentum effects might offset the thrust moment; pitching moment due to thrust was therefore removed for all further tests.

The oversensitive elevator posed a more serious problem. In the aircraft, low speed flight is normally performed with a 1:1 elevator gearing, but in the simulator it was thought that a gearing of 1·5:1 gave a response more akin to the aircraft than did the 1:1 gearing. In 1:1 gearing there was a marked tendency for pilot induced oscillations (PIOs), particularly immediately after take-off. A similar tendency to provoke a PIO on take-off is noted in the aircraft, but possibly not to the extent present in the simulator. No adequate explanation for the discrepancy could be found at the time and most of the simulator runs were performed with a 1·5:1 elevator gearing. One possible reason for the discrepancy could be the lack of full motion cues in the simulator; the absence of vertical acceleration cues means that the pilot relies on pitch rate and attitude cues from instruments, visual display and motion for his appreciation of the aircraft's response to his control movement. His awareness of the initial response of the aircraft will be reduced and there may be a tendency to apply more control than is required; overcontrol will only be apparent once a pitch rate has built up. The absence of vertical acceleration cues is likely to be particularly significant in the simulation of a small, responsive aircraft. A further simulation is planned shortly, to investigate the behaviour of a lateral autostabilizer to be fitted in the aircraft, and for this simulation heave as well as pitch motion will be available on the simulator cockpit, enabling some vertical acceleration cues to be provided.

A further possible source of error is the estimate of the aircraft's pitch inertia. Theoretical estimates of aircraft inertias, which are all that is available for the BAC 221, are frequently inaccurate; for example the measured pitch inertia of the FD2 aircraft (from which the BAC 221 was reconstructed) was found[10] to be 22 per cent higher than the theoretical estimate.

The elevator angles used for the take-off rotation in the simulator were higher than those used in the aircraft; this was consistent with the pilots' impressions of too great a nose-down pitching moment due to ground effect, so the effects of ground on pitching moment were halved for subsequent tests. With these reduced ground effects, the 1·5:1 elevator, and no pitching moment due to thrust, the pilots felt that a reasonable match between simulator and flight had been obtained.

The effects of negative speed stability during the landing approach were thought to be close to those encountered in flight. Speed control was not difficult, but close monitoring of airspeed was necessary to avoid speed excursions, and throttle inputs were more frequent than in conventional aircraft. Coarse use of throttle was required to restore the speed after an excursion. Fig. 5 shows throttle angle and airspeed for the final part of an approach in flight and simulator. There are frequent throttle inputs and in each case a thrust increase was required to check a speed divergence.

Approaches were performed at speeds up to 20 kt below the normal approach speed of 160 kt. Speed divergence was more rapid and even more attention was devoted to airspeed. At the approach speed of 140 kt, excursions of 10 kt were recorded. Speed reductions required sustained application of extra thrust to effect recovery to the nominal approach speed.

4.2. *Lateral Comparison.*

The lateral behaviour of the simulator was thought to be close to that of the aircraft; no changes to the simulation appeared necessary. The low speed handling exhibited the same problems that had been encountered briefly in flight, and further detailed investigation of some particular aspects was possible. These are discussed in section 7. Sidestep manoeuvres and cross-wind landings were performed for comparison with flight; these are analysed in detail in sections 5 and 6. The control usage and form of the sidestep manoeuvre were similar in simulator and flight, though smaller bank angles were used in the simulator runs. This may have been due to the roll motion cues used; since the motion system was driven in proportion to the aircraft's computed bank angle, large bank angles gave the sensations of large sideslips. The pilot was therefore inclined to use smaller bank angles to avoid unnatural motion cues. When, at a later stage of the simulation, a revised roll motion cue giving smaller false cues was tried, pilots freely used much larger bank angles during manoeuvres. However there was insufficient time available for any quantitative comparisons of the two motion cues.

4.3. *Simulation of Touchdown.*

In previous exercises on the Aero Flight simulator using the closed-circuit television display for outside-view representation, the pilot had been presented with the view by means of a television monitor placed above the instrument panel. Pilots criticised the quality of the display and said that, particularly during the final approach and flare, judgement of height and rate of descent was not as good as in actual flight. Touchdown rates of descent obtained in simulations of transport aircraft were far higher than experienced in real life.

For the present simulation, a projected television picture was used. Although the angular field of view of this system is unchanged from that of the monitor, it was hoped that greater realism would be obtained with the 'outside world' truly outside the cockpit.

The pilots who had used the monitor felt that although the quality of the projected picture was worse than that of the monitor, the impression of being surrounded by the world was much better and that judgement of height and rate of descent was better than with the monitor. Unfortunately there was no time available for comparison of the two forms of display with the same simulation.

Fig. 6 shows cumulative probability plots of rate of descent and touchdown point for the four Aero Flight pilots, and Fig. 7 presents the results as plots of touchdown point against rate of descent. Rates of descent are still higher than would be expected in real life (there are no flight measurements for com-

parison), but are an improvement over those obtained in previous simulations. In the simulation of Ref. 1 the 0·5 probability level of pilot A was 4·5 ft/sec; here, the same pilot achieved 2·5 ft/sec. The 0·5 level for all pilots combined was 5·3 ft/sec in Ref. 1, here it is 3 ft/sec and the highest level (pilot C) is only 4·2 ft/sec.

The improvement in touchdown performance obtained over previous simulations could be attributed to the new form of display or to the generally rapid response of the aircraft (previous simulations being of transport-type aircraft). However, a recent simulation of a large aircraft using the projected display has featured high touchdown rates, suggesting that the improvement was related to the aircraft response and not to the form of the display.

Differences in landing technique are noticeable among the pilots. Pilot B attempted to flare the aircraft with a single stick input, at about 20 ft wheel height, aimed at removing the rate of descent just above the ground; he then held attitude with the elevator and waited for the aircraft to sink to the ground as the speed decayed. His points in Fig. 7 show a tighter band of touchdown position close to the threshold than those of pilot A who sacrificed some distance in order to achieve lower touchdown rates of descent. His technique was to start a gentle flare at about 50 ft, progressively reduce the rate of descent until at about 10 ft and then to hold a low rate of descent until touchdown. The required accuracy of judgement of height and rate of descent required for the former technique is obviously greater and is reflected in the heavier touchdowns of pilot B; examination of records reveals touchdowns where the flare input was slightly too late, resulting in a heavy landing. The technique of pilot A is less demanding, as much of the rate of descent is removed before the aircraft is close to the ground. These differences in technique are illustrated in Fig. 8.

Both pilots had a number of hours experience of the real aircraft and both commented that they used the same landing technique in the simulator and in flight. Pilots C and D had not flown the aircraft prior to the simulation; in addition this was pilot C's first simulator exercise using a television display; his rates of descent and touchdown distances show more scatter than those of the other pilots.

5. *Sidestep Manoeuvres.*

Lateral displacement corrections during the final stages of a landing approach are conventionally achieved by a sidestep manoeuvre[11] in which the pilot performs an S-turn in order to align the aircraft with the runway centreline. Tomlinson[12] has shown that, for a slender-wing aircraft performing a sidestep in which the sideslip is suppressed by the use of rudder, the peak rudder angle required for the manoeuvre may be greater than the peak aileron angle. In addition, if sideslip is not suppressed, further aileron is required to overcome the large rolling moments due to sideslip. These theoretical studies of Ref. 12 used a specified bank angle time history and considered the control movements required to obtain the bank angle. Three time histories were used, and are shown in Fig. 9 along with the resulting lateral displacement time histories. A manoeuvre efficiency, E, was defined in Ref. 12, where

$$E = \frac{S}{S_o} \times 100\%,$$

S is the sidestep distance achieved and S_o is the distance that would result from the idealised bank angle function shown as curve D in Fig. 9 with the same peak bank angle and manoeuvre time.

Sidesteps were performed in the simulator for comparison with flight results. The pilot followed a laterally displaced ILS beam down to a cloudbase of 350–450 ft, and then, on breaking cloud, visually aligned the aircraft with the runway before touchdown.

Fig. 10 shows time histories of comparable sidestep manoeuvres in the aircraft and simulator (the sidestep being followed by an overshoot in the simulator run). There is a marked similarity between the two sets of traces, with a few detailed differences that are of interest. Aileron usages are comparable, but greater co-ordinating rudder inputs were used in the simulator, resulting in a less oscillatory bank angle trace at the peaks of the bank response. Elevator angles are, in the main, smaller in the simulator than in flight but around the middle of the simulator trace there are signs of some overcontrolling, prob-

ably induced as a result of unintentional elevator inputs during the large stick movements in roll. Airspeed and sideslip are smoother in flight traces than in the simulator due to instrumentation characteristics.

Manoeuvre times as a function of sidestep distance in the simulator are shown in Fig. 11 with some flight results from Ref. 13. Manoeuvre times in flight are consistently shorter than in the simulator; however, in neither flight nor simulator were pilots asked to perform the sidestep as quickly as possible and the bank angles used in the simulator were generally smaller. The incorrect sideforce cues during rolling of the simulator, mentioned in section 4, might have inhibited the pilots from using larger bank angles.

The bank angles used for the second part of the sidestep were generally less than those used for the first part. As the pilot has to perform the sidestep within a given distance along the ground (i.e. before the runway threshold) he tends to make a rapid roll into the sidestep, and then 'tailor' the rest of the manoeuvre to fit into the available distance. This will lower the 'efficiency' of the manoeuvre (as defined above). Fig. 12 shows the manoeuvre efficiencies for simulator and flight as a function of the ratio of the smaller to the larger bank angles. Also shown are the efficiencies of the theoretical manoeuvres A, B and C. As the bank angle ratio tends towards 1·0 the efficiency of flight and simulator manoeuvres tends to about 60 per cent, a little worse than curve A.

These results are presented in an alternative form in Fig. 13 where the peak bank angle divided by the sidestep distance is plotted against manoeuvre time. Curves derived from the theoretical manoeuvres A, B and C are also shown; the results for both simulator and flight are grouped around curve B with the more efficient points approaching curve A. Thus a manoeuvre efficiency somewhere between those of A and B could be assumed to predict the peak bank angles required for a given sidestep distance in a given time.

If the method is extended to a comparison of peak aileron angles the results are as shown in Fig. 14. Peak control movements are much greater than predicted by even the least efficient of the three curves (curve C), simulator and flight angles exceeding curve C by similar amounts. However, the control angles predicted by curve C are small (2–3°) for the size of sidestep performed here, and the pilot has ample control available (10° at an aileron gearing of 2:1); the ailerons were usually applied as short inputs of moderate amplitude rather than as smooth, continuous and small inputs. For estimating the amount of aileron required to perform a given sidestep one ought, perhaps to consider the more economical, in terms of aileron usage, of the sidesteps performed as a guide to what can be achieved; manoeuvre C then appears to be a suitable measure of the aileron angle required for sidesteps.

The manoeuvre shown in Fig. 15a is one in which rudder has been used to suppress sideslip. If co-ordinating rudder is not used, an oscillatory roll response results, as in Fig. 15b. These two sidesteps are identified in Figs. 11 and 12 as points (a) and (b); it can be seen that run (b) (no rudder) has a low efficiency and high manoeuvre time. Nearly all simulator and flight sidesteps were performed with the aid of rudder, so a detailed analysis of the effects of rudder is not possible, but theoretical calculations show that 50 per cent to 100 per cent more rudder than aileron would be required to suppress sideslip completely.

6. *Crosswind Landings.*

In a conventional crosswind approach and landing a crabbing technique is used in which the aircraft heads partially into wind with wings level so that the resulting track over the ground is along the extended runway centreline. Just before touchdown it is necessary to yaw the aircraft so that its heading is approximately aligned with the track to give an acceptable lateral drift at the wheels at touchdown. This exposes the aircraft to the crosswind and with a slender-wing aircraft having relatively high yaw inertia (and hence a significant time of exposure to the crosswind), high roll response to sideslip, low roll inertia and low roll damping there will be a significant response in roll unless checked by the ailerons.

An alternative approach technique, little used, is the sideslipping method in which the aircraft's heading is aligned with the runway, and a sideslip into wind is maintained so that the track is again along the

extended centreline. At touchdown it is only necessary to roll the aircraft to wings level, a more rapid and easily controlled manoeuvre which does not expose the aircraft to an appreciable change in sideslip angle. However, rudder and aileron are required to maintain the sideslip and it is a less comfortable approach technique, leaving the pilot less reserve lateral control in one direction for the control of response to turbulence and for manoeuvres.

Crosswind landings using the crabbing approach technique have been performed in flight with the BAC 221 and are reported in Ref. 13. The crab angles required for the crosswinds experienced (up to 12 kt) were relatively small (less than $4\frac{1}{2}°$) and there was no need to kick-off the drift.

In the simulator the pilots were asked to remove the drift so that the possible hazards associated with the build-up of sideslip could be studied. Fig. 16 shows time histories of approaches in a 12 kt crosswind in flight and simulator; lateral control inputs are generally similar. The rudder angles required to remove drift just before touchdown are small and there is little resulting sideslip apparent in flight; an increase in sideslip is visible in the simulator trace. The aileron and rudder angles used during the kick-off drift phase are little different from those required to control the aircraft on the approach in the level of turbulence associated with the crosswind. In both flight and simulator, near-zero bank angle is achieved at touchdown.

Fig. 17 shows the rudder angles used to kick-off drift, and the aileron angles applied to oppose the resulting rolling moment, for all the simulator crosswind landings. Also indicated are the control angles required to maintain a steady sideslip appropriate to the crosswind strength for an airspeed of 160 kt (approach speed) and 145 kt (typical touchdown speed). Aileron angles required are generally less than or close to the values required for a steady sideslip. On one occasion the aileron angle is substantially greater than that required for the sideslip and is close to the maximum available aileron angle of 10° at the gearing of 2:1 used for these approaches; in this run the pilot applied excessive rudder and yawed 2° beyond the no-drift heading.

A single slipping approach was performed; the peak control angles are plotted in Fig. 17; the maximum aileron angle used was large and in excess of the typical angles used for the crabbing approach. Fig. 18 illustrates this slipping approach and a conventional crabbed approach performed by the same pilot; for both approaches the crosswind strength was 15 kt. In the slipping approach the pilot changes from the crabbed to the slipping technique at about 400 ft to reduce the time spent with crossed controls. The pilot found control of the aircraft in roll very unpleasant; it was difficult to control the aircraft's roll response to the turbulence whilst holding on the aileron and rudder deflections required for the sideslip, and an oscillation in roll resulted. The technique was thought unsuitable for an aircraft with such a rapid response to disturbances in roll and adverse reaction to sideslip.

The deficiencies of the visual display were found to affect the judgement of the kick-off drift phase of the crabbing approach. It took about five seconds for the aircraft to yaw to the required heading but it was then necessary to touch down immediately or the aircraft would start to drift across the runway. Pilots were unable to estimate the touchdown point and were thus not sure of when to kick-off the drift. Fig. 18a shows an approach in which a substantial amount of drift is removed, but touchdown did not occur for another $3\frac{1}{2}$ seconds and the drift angle had built up again. Drift angles at touchdown experienced in the simulator were occasionally larger than the drift angle on the approach. The high inertia in yaw and hence the slow yaw response is obviously a contributory factor to the difficulty of accurately kicking off drift but the quality of the visual display precludes a detailed study of the touchdown phase of crosswind landings.

7. *Lateral Control Problems in High Incidence Flight.*

One characteristic of the lateral behaviour of the BAC 221 at high incidence is that the lateral modes of motion (with controls fixed) retain stability beyond the incidence at which the directional stability derivative n_v becomes negative. However, in flight tests at incidences where n_v should be close to zero, and at which the lateral modes were expected to be stable, some control difficulty was encountered which appeared to be associated with directional instability. A flight record of this condition is shown in Fig. 19a, revealing an oscillation of about 15 seconds period.

The disagreement between classical stability analysis and flight experience prompted a theoretical investigation of control of the aircraft[14], in which it was assumed that the pilot used the ailerons so that the bank angle was perfectly constrained to wings-level flight. It was found that such a mode of control would result in a directional divergence when the effective derivative $\bar{n}_v (= n_v - l_v n_\xi / l_\xi)$ became negative; this would be at an incidence about 4° lower than that at which n_v changes sign (for n_v in aerodynamic body axes). Thus although the uncontrolled motion of the aircraft is stable, control of bank angle by use of aileron can lead to instability.

The theoretical calculations used wind tunnel estimates of the aircraft derivatives, and in the absence of measured derivatives from flight results, accurate correlation of theory and flight experience was not possible. However, the simulator was 'flown' with known derivatives and hence further study could be undertaken. Flight at incidence comparable to the real flight conditions was attempted in the simulator and similar encounters with control difficulties were experienced (Fig. 19b). The test conditions in flight and simulator were different; the flight tests were performed at 25000 ft altitude and the simulator tests at sea level conditions. The unsuitability of the visual display for the simulator task (high pitch attitude and hence very restricted forward view, and large heading changes) meant that the simulator tests were performed under instrument flight conditions.

The simulator behaviour differed from flight in that quite large bank angles were present (possibly due to the lack of external visual reference); also in both flight and simulator appreciable amounts of rudder were used and hence the concept of perfect constraint of bank angle by aileron alone is hardly valid. This stimulated some theoretical calculations on the effect of relaxing the constraint on bank angle. The following discussion relates to the aircraft in the clean configuration, and is strictly only valid for sideslip angles less than 3° (as n_v is non-linear).

Fig. 20a shows the lateral stability roots of the unconstrained aircraft as a function of incidence (measures of period and damping are also indicated). The Dutch roll oscillation is well damped with a period of around 3 seconds. The roll and spiral modes are subsidences up to around 21° incidence, when they combine to give a second oscillation; at 24° this oscillation has a period of 14 seconds and is well damped; the time to half amplitude ($T\frac{1}{2}$) is 4 seconds.

When bank angle is perfectly constrained by the use of ailerons the equation determining the stability degenerates into a quadratic, giving the roots shown in Fig. 20b. Up to about 21·5° incidence the solution is oscillatory, with a $T\frac{1}{2}$ of around 4 seconds; at higher incidence the roots are aperiodic and one moves into the right-hand half of the plane, giving a divergence. The reason for the divergence can be seen simply if the response of the aircraft to an aileron step is considered. Adverse yaw from the outboard aileron will produce a moment ($n_\xi \xi$) generating sideslip. The sideslip produces an opposing moment ($-n_v \beta$) and the balance of these terms gives $\beta = -(n_\xi / n_v)\xi$. Now the rolling moment due to this sideslip will be $l_v \beta = l_v(-n_\xi / n_v)\xi$ and if this term is greater than the rolling moment due to the ailerons ($l_\xi \xi$) the aircraft will roll the wrong way as sideslip builds up, though initial roll will be in the required direction. Further aileron application in the 'conventional' direction to oppose this roll will aggravate the situation, giving further roll in the wrong sense. Hence for stability we require $l_\xi \xi > (l_v n_\xi \xi)/n_v$, i.e. $n_v - l_v n_\xi / l_\xi > 0$, the criterion of Ref. 14.

The roll reversal resulting from aileron control can be seen in Fig. 21a–e where the response of the aircraft to a step aileron input is shown at various incidences. The values of $(l_\xi / l_v)\xi$ is marked; when sideslip exceeds this value, the rolling moment due to the sideslip is greater than that from the ailerons. Above 21·5° incidence the aircraft eventually rolls the wrong way in response to aileron, though the initial motion is in the right direction. Interconnection of rudder to aileron, so that aileron applies some rudder of the same sign, will add a negative component to the effective n_ξ (as n_ζ is negative) and hence will give an improvement in the value of $\bar{n}_v$. Fig. 21f and g show the effect of applying a simultaneous step of aileron and rudder; bank reversal is now avoided until a higher incidence.

Root locus techniques[15] can be used to consider the effect of relaxation of the bank angle constraint. If the aircraft transfer function for bank angle response to aileron is $\phi/\xi = G(s)$ and a pilot transfer function $\xi/\phi = KH(s)$ is assumed, the roots of the equation $1 + KG(s)H(s) = 0$ determine the stability of the pilot-aircraft closed loop system. The root locus method plots the locus of the roots of the equation

as the pilot's gain K increases from zero (where the roots are known as the 'poles') to infinity (the 'zeros'). The roots of the uncontrolled aircraft motion will appear as poles of the diagram. As mentioned earlier, the control difficulties experienced in the simulator were under conditions some way removed from that of perfect bank angle constraint using aileron; in particular, bank angles were appreciable and rudder was used to supplement aileron control. The perfect constraint approach predicts an oscillation with $T_{\frac{1}{2}}$ of around 4 seconds—quite well damped—changing above 21·5° incidence to a divergence (Fig. 20b). At the time of the oscillation shown in Fig. 19b the incidence was about 23·5°, well above the incidence for divergence predicted by perfect constraint, and the oscillation appears almost neutrally damped. The root locus technique illustrates possible reasons for the differences.

Fig. 22a shows a root locus plot for $\alpha = 24°$, assuming that the pilot reacts to bank angle and roll rate with a transfer function of the form $\xi/\phi = KH(s) = K(2+s)$. This simple representation of the pilot, while by no means accurate, is sufficient to illustrate the features of interest in control of the aircraft. The zero at -2 is the only pole or zero that is dependent on the pilot transfer function; all others are derived from the aircraft transfer function and hence changes in the pilot representation should not effect the loci to too great an extent.

As one would expect, the roots from the 'second oscillation' of the controls-fixed aircraft combine to give zeros corresponding to the roots for the perfect constraint theory as the pilot's gain is increased. However for all gains where the mode is still oscillatory there is a $T_{\frac{1}{2}}$ of around 4 seconds; relaxation of bank angle constraint does not produce a neutrally damped oscillation.

Fig. 22b shows the effect of gearing the rudder to the ailerons so that rudder angle exactly equals aileron angle. Increasing pilot gain no longer results in a divergence; the roots remain stable for all gains. Conditions intermediate between those of Fig. 22a and b are illustrated in Fig. 23 which shows the loci of the zeros of the aircraft transfer function for various values of aileron to rudder gearing G; a gearing of $\frac{1}{2}$ is sufficient to prevent divergence at this incidence.

It is now of interest to consider the effects of lags on the plots discussed. The effect of introducing lags into the pilot transfer function would be to give further poles on the real axis in Fig. 22a and b; however the aircraft transfer function poles and zeros will be unchanged and there will be little shift in the overall plot. A different picture emerges if we assume that the rudder inputs lag behind the aileron movement. Fig. 24 shows the plot when the rudder lags aileron by one second with a rudder-aileron ratio of 1 (which is of the order of the rudder-aileron ratio used by pilots in the simulator). The complex zeros of the aircraft transfer function have now moved into the right-hand side of the diagram, giving an unstable oscillation. Fig. 25 gives the effect on the position of these zeros of varying the rudder lag. These zeros, of course, define the roots for infinite pilot gain. A typical value of the actual pilot gain would give a root approximately midway along the line joining the appropriate zero to the second oscillation complex pole. Thus a lag of about 1 second between rudder and aileron would give an oscillation which is close to neutrally damped and of period similar to the second oscillation period. This oscillation is typical of that met in flight and simulator. Such a relatively small lag of rudder behind aileron could easily result from the pilot applying rudder to remove the sideslip caused by the adverse aileron yaw, rather than applying simultaneous aileron and rudder.

Bank angle control on rudder alone was found to be possible, but accuracy of control was poor. Thus for accurate bank angle control at high incidence, accurate and lag-free interconnection of rudder and aileron is necessary; the pilot would be unable to supply the close phasing required. Fig. 26 illustrates this clearly; for the first portion of the traces the pilot is using quite large rudder angles approximately in phase with the ailerons, but the long period oscillation still persists. Then the interconnect giving $\zeta = \xi$ is engaged and the pilot stops applying rudder; the oscillation disappears immediately.

A further feature of the traces of Figs. 19 and 26 is the presence of a short period oscillation of higher frequency than the dutch roll mode. The root locus plots would suggest that this is due to the pilot's mode of control of the dutch roll; an increase of gain initially gives an increase in frequency of the roots associated with the dutch roll. A typical pilot gain would give roots in the region of the points AA′ in Fig. 24; the period of this mode would be about $2\frac{1}{2}$ seconds as compared with the dutch roll period of $3\frac{1}{2}$ seconds.

The root locus method has thus suggested reasons for the form of the lateral control difficulties experienced on the BAC 221 in flight at high incidence, and has emphasised the need for close phasing between aileron and rudder inputs. This control difficulty is not confined to this aircraft and may appear on other slender aircraft with similar adverse aileron yaw characteristics.

8. *Discussion and Simulator Validation.*

8.1. *Representation of the BAC 221.*

In the absence of flight measurements of aircraft derivatives, assessment of the accuracy of the simulation must rest largely on pilots' judgements of the similarity of aircraft and simulator. These judgements were hampered somewhat by the length of time since the aircraft had last flown. However, pilots felt that in general a satisfactory simulation had been achieved and that the handling features which characterised the aircraft were well represented. Of the two major deficiencies, that of oversensitive response to elevator has not been resolved but may be attributable to incorrect inertia values or to insufficient motion cues. The second deficiency, the inability to provide an accurate simulation of touchdown, demands improvements beyond the present state of the art of visual displays for simulation. Some doubt was also expressed as to the accuracy of the ground effect representation which, though judgement here was inevitably influenced by the quality of the visual simulation of touchdown, is a common area of uncertainty in wind tunnel data.

Comparisons of flight and simulator traces of particular manoeuvres were favourable, and control usage during sidestep manoeuvres appeared similar in flight and simulator although the incomplete simulator motion cues may have limited the rapidity of the manoeuvres. A close comparison of flight at high incidence was achieved and further insight gained into the lateral control problems at this condition.

8.2. *Relevance to Previous SST Simulation.*

It is obvious that the sizes of the BAC 221 and the SST are widely different and hence the time scales of the dynamic modes of the two aircraft are dissimilar.

However there is much in common in their lateral modes of motion, particularly when considering the unstabilised SST, when the oscillatory roll behaviour predominates. With stabilisation there is an increase in roll damping and hence smoother roll control and less response to gusts. The behaviour of the two aircraft under conditions of negative speed stability (i.e. with autothrottle failed for the SST) should also be similar. In view of these factors the satisfactory simulation of lateral behaviour and of the effects and control of the speed instability is encouraging. In the longitudinal plane there were problems during touchdown with the SST; similar difficulties were encountered in this simulation, highlighting the need for improved visual representation of this phase of simulated flight.

9. *Conclusions.*

A piloted flight simulator study of the BAC 221 slender-wing research aircraft was performed and qualitative comparison of the simulator with the real aircraft was made by test pilots familiar with the aircraft. The lateral behaviour of the simulator was considered to be close to that of the aircraft, as were speed control and the effects of negative speed stability. The longitudinal response to elevator was considered high; the explanation for this discrepancy has not been found, but may be associated with too low an inertia in pitch or insufficient motion cues. A further simulation to be performed shortly with better motion cues may resolve the problem. The effect of ground proximity on the simulated aerodynamics appeared too large, and was reduced for the main test programme. Pitching moments due to thrust changes were thought excessive and were removed.

Sidestep manoeuvres and crosswind landings were performed; control usage during sidesteps was similar in flight and simulator, and the need for co-ordinating rudder to suppress sideslip was observed. Sidesteps without rudder were possible, but the build-up of sideslip led to an oscillatory roll response. The sideslipping method of crosswind approach was found to be unsuitable; detailed study of the kick-off drift phase of the crabbed approach method was limited by the inadequacies of the visual display.

The quality of the view presented to the pilot was insufficient for accurate judgement of height and rate of descent close to the ground and difficulty was experienced in kicking-off drift at the right time. The poor height and rate of descent cues also led to touchdown rates of descent greater than those experienced in real flight.

In simulation of flight at high incidence, lateral control difficulties similar to those met in flight were encountered. It was found necessary for rudder to be applied closely in phase with aileron in order to overcome adverse aileron yaw and suppress the instability resulting from tight aileron control of bank angle. Theoretical calculations using the root locus method showed that a lag of one second between rudder and aileron was sufficient to affect the aircraft handling significantly.

The degree of success of the simulation inspired confidence in much of the previous simulation of a slender-wing supersonic transport aircraft, but improvements to the quality of visual representation are required before a successful simulation of the final stages of an approach and landing is possible.

LIST OF SYMBOLS

b	Reference wing span
$\bar{c}$	Reference chord
C_L, C_D, C_Y	Aerodynamic force coefficients
C_l, C_m, C_n	Aerodynamic moment coefficients, defined as $C_l = \frac{L}{\frac{1}{2}\rho V^2 Sb}$ $C_m = \frac{M}{\frac{1}{2}\rho V^2 S\bar{c}}$ $C_n = \frac{N}{\frac{1}{2}\rho V^2 Sb}$
E	Sidestep manoeuvre efficiency
$f(\alpha)_c f(\alpha)_A$	Incidence functions defined in Appendix
g	Acceleration due to gravity
G	Aileron-rudder interconnect gearing
$G(s)$	Aircraft transfer function of bank angle response to aileron
$H(s)$	Pilot transfer function of aileron as a result of bank angle
h_{cg}	Height of centre of gravity above ground
h_G	Ground height parameter, $h_G = h_{cg} + 0{\cdot}75$ ft
Ixx, Iyy, Izz	Moments of inertia with respect to principal axes
K	Constant in pilot transfer function
L, M, N	Aerodynamic moments
l_p, l_r	Moment derivatives, defined in Appendix
l_v	Rolling moment derivative due to sideslip
l_ξ	Rolling moment derivative due to aileron
n_p, n_r	Moment derivatives, defined in Appendix
n_v	Yawing moment derivative due to sideslip
$\bar{n}_v$	Effective yawing moment derivative due to sideslip, see section 6

n_ξ	Yawing moment derivative due to aileron
p, q, r	Angular velocity components
s	Laplace variable
s	Sidestep distance
s_o	Theoretical maximum sidestep distance
S	Reference wing area
t	Time
T	Sidestep manoeuvre time
V	Airspeed
y	Lateral displacement
α	Angle of incidence
β	Angle of sideslip
ε	Inclination of principal axes to body datum
ζ	Rudder angle
η	Elevator angle
ξ	Aileron angle
ρ	Air density
ϕ	Bank angle
ϕ_1, ϕ_2	Peak bank angles for first and second parts of sidestep manoeuvre

LIST OF REFERENCES

No.	Author(s)	Title, etc.
1	B. N. Tomlinson and T. Wilcock	Further piloted simulation studies of the handling characteristics of a slender-wing supersonic transport aircraft during approach and landing. A.R.C. R. & M. 3660 (1969).
2	B. N. Tomlinson and T. Wilcock	A piloted simulation of the take-off of a supersonic transport aircraft, with and without a take-off director. A.R.C. R. & M. 3594 (1967).
3	C. S. Barnes and O. P. Nicholas	Preliminary flight assessment of the low-speed handling of the BAC 221 ogee-wing research aircraft. A.R.C. C.P. 1102 (1967).
4		Type 221 Model A. Stability and control tests at high incidence and with ground effect. B.A.C. (Filton) Report W.T. 488.
5		Unpublished results of BAC 221 model tests in the R.A.E. 13ft × 9ft wind tunnel.
6	W. J. G. Pinsker	'Zero rate of climb speed' as a low speed limitation for the stall-free aircraft. A.R.C. CP 931 (1966).
7	T. Wilcock	Piloted simulator investigations of flight near zero rate of climb speed. R.A.E. Technical Report 70016 A.R.C. 32 171 (1970).
8	D. H. Perry, L. H. Warton and C. E. Welbourn	A flight simulator for research into aircraft handling characteristics. A.R.C. R. & M. 3566 (1966).
9	R. Rose and C. S. Barnes	Some flight and wind tunnel longitudinal stability measurements on the BAC 221 slender-wing aircraft. R.A.E. Technical Report 70054 A.R.C. 32 330 (1970).
10	C. S. Barnes and A. A. Woodfield	Measurements of the moments and product of inertia of the Fairey Delta 2 aircraft. A.R.C. R. & M. 3620 (1968).
11	D. H. Perry, W. G. A. Port and J. C. Morrall	A flight study of the sidestep manoeuvre during landing. A.R.C. R. & M. 3347 (1961).
12	B. N. Tomlinson	An extensive theoretical study of the ability of slender-wing aircraft to perform sidestep manoeuvres at approach speeds. A.R.C. R. & M. 3359 (1962).
13	F. W. Dee, R. Rose and O. P. Nicholas	Brief flight tests of crosswind landings and sidestep manoeuvres on the BAC 221 aircraft. R.A.E. Technical Report 68251 (A.R.C. 30959) (1968).
14	W. J. G. Pinsker	Directional stability in flight with bank angle constraint as a condition defining a minimum acceptable value for n_v. A.R.C. R. & M. 3556 (1967).
15	W. R. Evans	*Control system dynamics.* McGraw Hill Book Co., New York, 1954.

APPENDIX

Aircraft Data as Used in the Simulation.

A.1. *Dimensions, weight, etc.*

Reference wing area S	490 ft^2
Reference wing chord $\bar{c}$	25 ft
Reference wing span b	25 ft
Reference *cg* point	
clean configuration	161 inches forward of datum
approach configuration	159 inches forward of datum
Pilot's eye position	375 inches forward of datum and 25 inches above datum
Weight	18500 lb
Undercarriage:	
bottom of main wheel tyres for oleos fully extended	122 inches forward of datum and 95 inches below datum
bottom of nosewheel tyres for oleo fully extended	345 inches forward of datum and 122 inches below datum
Rolling inertia with respect to principal axes, Ixx	
clean configuration	$0{\cdot}73 \times 10^4$ slug ft^2
approach configuration	0.91×10^4 slug ft^2
Pitching inertia with respect to principal axes, Iyy	
clean configuration	5.07×10^4 slug ft^2
approach configuration	5.41×10^4 slug ft^2
Yawing inertia with respect to principal axes, Izz	
clean configuration	5.69×10^4 slug ft^2
approach configuration	5.94×10^4 slug ft^2
Body datum x-axis is inclined ε nose up relative to x principal axis where	
for clean configuration	$\varepsilon = 0° 40'$
for approach configuration	$\varepsilon = 1° 18'$
Maximum net thrust	8000 lb

Thrust response to throttle shaped to give 6 seconds from idle to full thrust in response to full throttle.

A.2. *Aerodynamic coefficients—clean configuration.*

(a) *Longitudinal* (aerodynamic-body axes)

Lift coefficient $C_L = 0{\cdot}0360\alpha + 0{\cdot}0108\alpha_{L22{\cdot}5°} - 0{\cdot}0278f(\alpha)_c + 0{\cdot}0093\eta + 0{\cdot}00015\alpha\eta$.

Drag coefficient $C_D = 0{\cdot}00387 - 0{\cdot}001823\alpha + 0{\cdot}000729\alpha^2 + 0{\cdot}00023\alpha\eta - 0{\cdot}00046\eta$.

Pitching moment coefficient $C_m = 0{\cdot}00956 - 0{\cdot}003387\alpha + 0{\cdot}000152\alpha^2 - 0{\cdot}000003075\alpha^3 + 0{\cdot}0061f(\alpha)_c - 0{\cdot}00353\eta$

K

where α and η are in degrees

$f(\alpha)_c = 0$ for $\alpha < 21{\cdot}5°$
$= 1$ for $\alpha > 22{\cdot}5°$
$= (\alpha - 21{\cdot}5°)$ for $21{\cdot}5° < \alpha < 22{\cdot}5°$
$\alpha_{L22{\cdot}5} = \alpha$ for $\alpha < 22{\cdot}5$
$= 22{\cdot}5$ for $\alpha > 22{\cdot}5$.

$$\text{Damping in pitch } \frac{\partial C_m}{\partial\left(\frac{q\bar{c}}{V}\right)} = -0{\cdot}194 \text{ per radian}$$

$$\frac{\partial C_m}{\partial\left(\frac{\dot{\alpha}\bar{c}}{V}\right)} = -0{\cdot}096 \text{ per radian}.$$

(b) *Lateral* (body axes—x-axis along aircraft datum)

Sideforce coefficient $C_y = -0{\cdot}0068\beta + 0{\cdot}0013\zeta$.
Roll coefficient $C_l = -0{\cdot}000759\beta - 0{\cdot}00228\beta_{L\pm 5°} - 0{\cdot}00131\xi$.
Yaw coefficient $C_n = 0{\cdot}0013\beta - 0{\cdot}00022[\alpha - 18]_{L+ve}\beta$
$- 0{\cdot}00018[\alpha - 18]_{L+ve}\beta_{L\pm 3°}$
$+ 0{\cdot}000018\alpha\xi - 0{\cdot}00046\xi - 0{\cdot}00086\zeta$

where α, β, ζ and ξ are in degrees

$\beta_{L\pm 5°} = -5$ for $\beta < -5$
$= \beta$ for $-5 < \beta < +5$
$= +5$ for $\beta > +5$
$\beta_{L\pm 3°}$ is similarly defined
$[\alpha - 18]_{L+ve}$ indicates that the term takes the value 0 for $\alpha < 18°$.

$$\text{Rolling moment due to rate of roll } l_p = \frac{\partial C_l}{\partial\left(\frac{pb}{2V}\right)} = -0{\cdot}27 \text{ per radian}$$

$$\text{Rolling moment due to rate of yaw } l_r = \frac{\partial C_l}{\partial\left(\frac{rb}{2V}\right)} = -0{\cdot}0593 + 0{\cdot}0748\alpha - 0{\cdot}0675\alpha_{L20{\cdot}5°} \text{ per radian}$$

$$\text{Yawing moment due to rate of roll } n_p = \frac{\partial C_n}{\partial\left(\frac{pb}{2V}\right)} = -0{\cdot}082 + 0{\cdot}0684\alpha - 0{\cdot}0636\alpha_{L20{\cdot}5°} \text{ per radian}$$

$$\text{Yawing moment due to rate of yaw } n_r = \frac{\partial C_n}{\partial\left(\frac{rb}{2V}\right)} = -0{\cdot}296 - 0{\cdot}088\alpha + 0{\cdot}088\alpha_{L20{\cdot}5°} \text{ per radian}$$

where α is in degrees
and $\alpha_{L20{\cdot}5}$ is defined similarly to $\alpha_{L22{\cdot}5}$ above.

A.3. *Aerodynamic coefficients—approach configuration*

(a) *Longitudinal* (aerodynamic-body axes)

$$\text{Lift coefficient } C_L = 0{\cdot}0303\alpha + 0{\cdot}0075\alpha_{L21{\cdot}5^\circ} - 0{\cdot}0627 - 0{\cdot}0314 f(\alpha)_A + \frac{1}{h_G}(0{\cdot}140\alpha - 0{\cdot}411 + 0{\cdot}016\eta) + 0{\cdot}0079\eta + 0{\cdot}00014\alpha\eta\,.$$

$$\text{Drag coefficient } C_D = 0{\cdot}0307 + 0{\cdot}000024\alpha + 0{\cdot}0005417\alpha^2 + \frac{1}{h_G}(0{\cdot}002314\alpha^2 - 0{\cdot}01224\alpha) + 0{\cdot}00023\alpha\eta - 0{\cdot}00046\eta\,.$$

$$\text{Pitching moment coefficient } C_m = -0{\cdot}0042 - 0{\cdot}001535\alpha + 0{\cdot}0001132\alpha^2 - 0{\cdot}00000239\alpha^3 + 0{\cdot}0059 f(\alpha)_A + \frac{1}{h_G}(0{\cdot}1678 - 0{\cdot}0215\alpha) - 0{\cdot}00322\eta$$

where α and η are in degrees

$f(\alpha)_A = 0$ for $\alpha < 20{\cdot}5^\circ$

$= 1$ for $\alpha > 21{\cdot}5^\circ$

$= (\alpha - 20{\cdot}5)$ for $20{\cdot}5^\circ < \alpha < 21{\cdot}5^\circ$

$h_G = h_{cg} + 0{\cdot}75$ ft where h_{cg} = height of centre of gravity above ground and h_G is limited to a maximum value of 25 ft

$\alpha_{L21{\cdot}5}$ is defined similarly to $\alpha_{L22{\cdot}5}$ in the clean configuration.

$$\text{Damping in pitch } \frac{\partial C_m}{\partial\left(\frac{q\bar{\bar{c}}}{V}\right)} = -0{\cdot}172 \text{ per radian}$$

$$\frac{\partial C_m}{\partial\left(\frac{\dot{\alpha}\bar{\bar{c}}}{V}\right)} = -0{\cdot}086 \text{ per radian}.$$

(b) *Lateral* (body axes)

$$\text{Sideforce coefficient } C_Y = -0{\cdot}0096\beta + 0{\cdot}0009\zeta$$

$$\text{Roll coefficient } C_l = -0{\cdot}001481\beta - 0{\cdot}000524\beta_{L\pm5^\circ} - 0{\cdot}00155\zeta$$

$$\text{Yaw coefficient } C_n = 0{\cdot}000273\beta + 0{\cdot}000026\alpha\xi - 0{\cdot}00044\xi - 0{\cdot}00075\zeta$$

where α, β, ξ and ζ are in degrees

and $\beta_{L\pm5^\circ}$ is defined as for the clean configuration.

Damping derivatives:

$l_p = -0{\cdot}237$ per radian

$l_r = -0{\cdot}0529 + 0{\cdot}0615\alpha - 0{\cdot}0521\alpha_{L20{\cdot}5}$ per radian

$n_p = -0{\cdot}082 + 0{\cdot}047\alpha - 0{\cdot}040\alpha_{L20{\cdot}5}$ per radian

$n_r = -0{\cdot}410$ per radian

where α is in degrees and $\alpha_{L20{\cdot}5}$ is defined as for the clean configuration.

A.3. *Controls*

Maximum control movements were elevator (η) $+15°$ to $-25°$
aileron (ξ) $\pm 20°$
rudder (ζ) $\pm 15°$

Aileron and elevator sensitivities could be varied by a gearing selector giving reduced control surface travel for a given stick deflection

Available gearing were:— elevator 1:1, 1·5:1, 2:1
aileron 1:1, 2:1, 4:1

(In the aircraft, gearing is continuously variable over the range 1:1 to 9:1 for elevator and 1:1 to 6:1 for aileron.)

An interconnect between aileron and rudder was sometimes used, giving a rudder angle $\zeta° = [10_S/(1 + 10_S)]\zeta°$. The applied rudder was limited to ± 5.

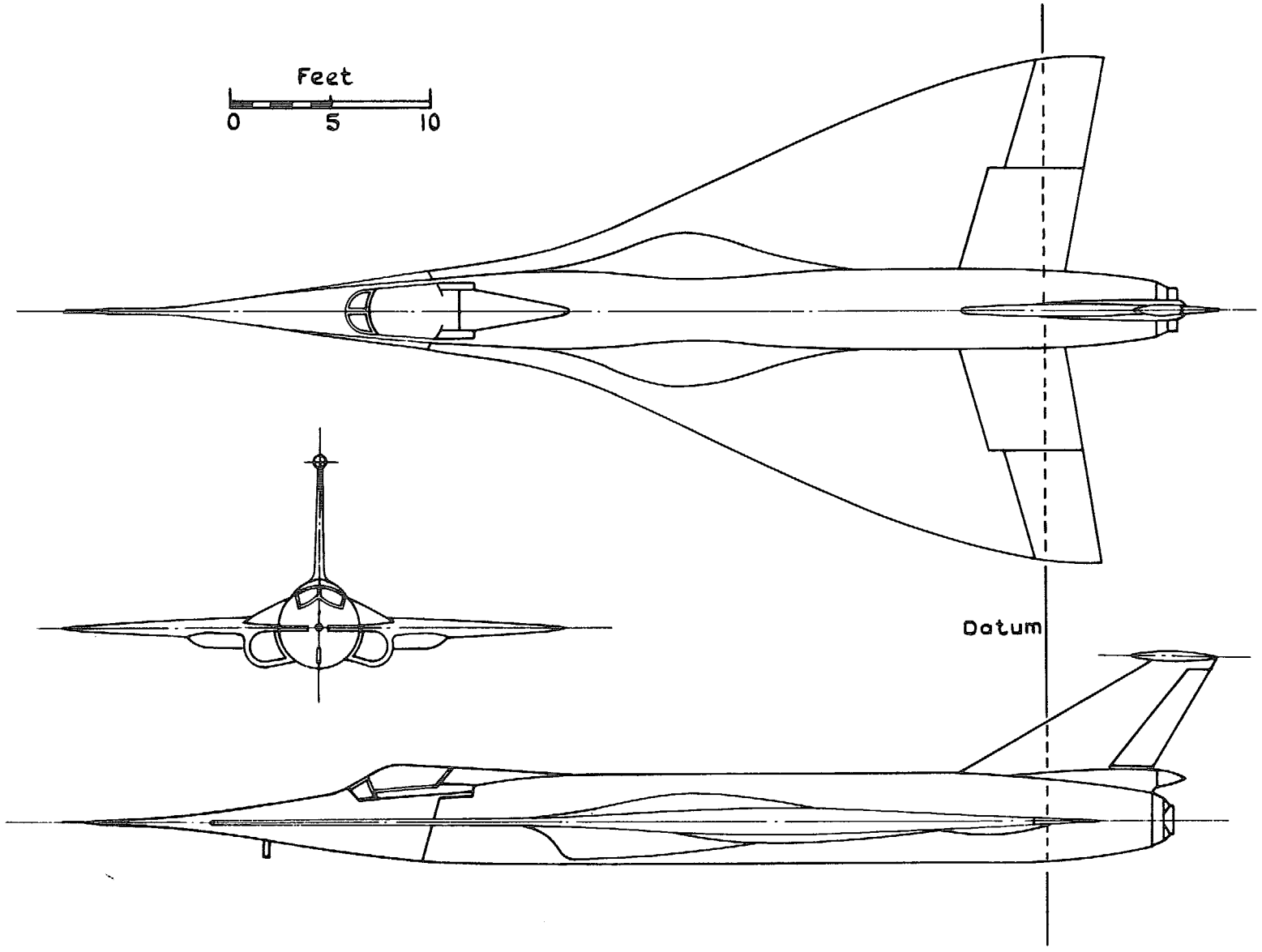

FIG. 1. BAC 221 General arrangement.

FIG. 2. View of BAC 221 in approach configuration.

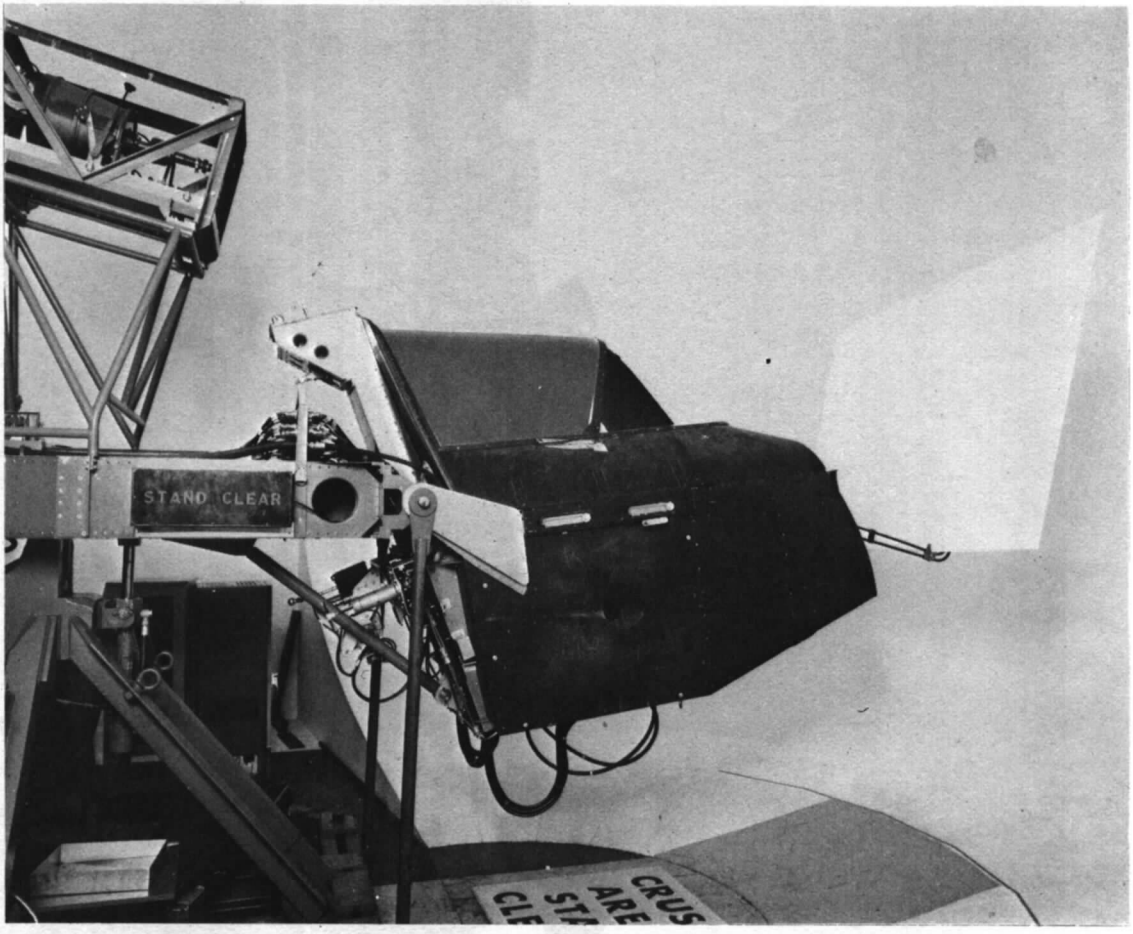

FIG. 3. Simulator cockpit and motion system.

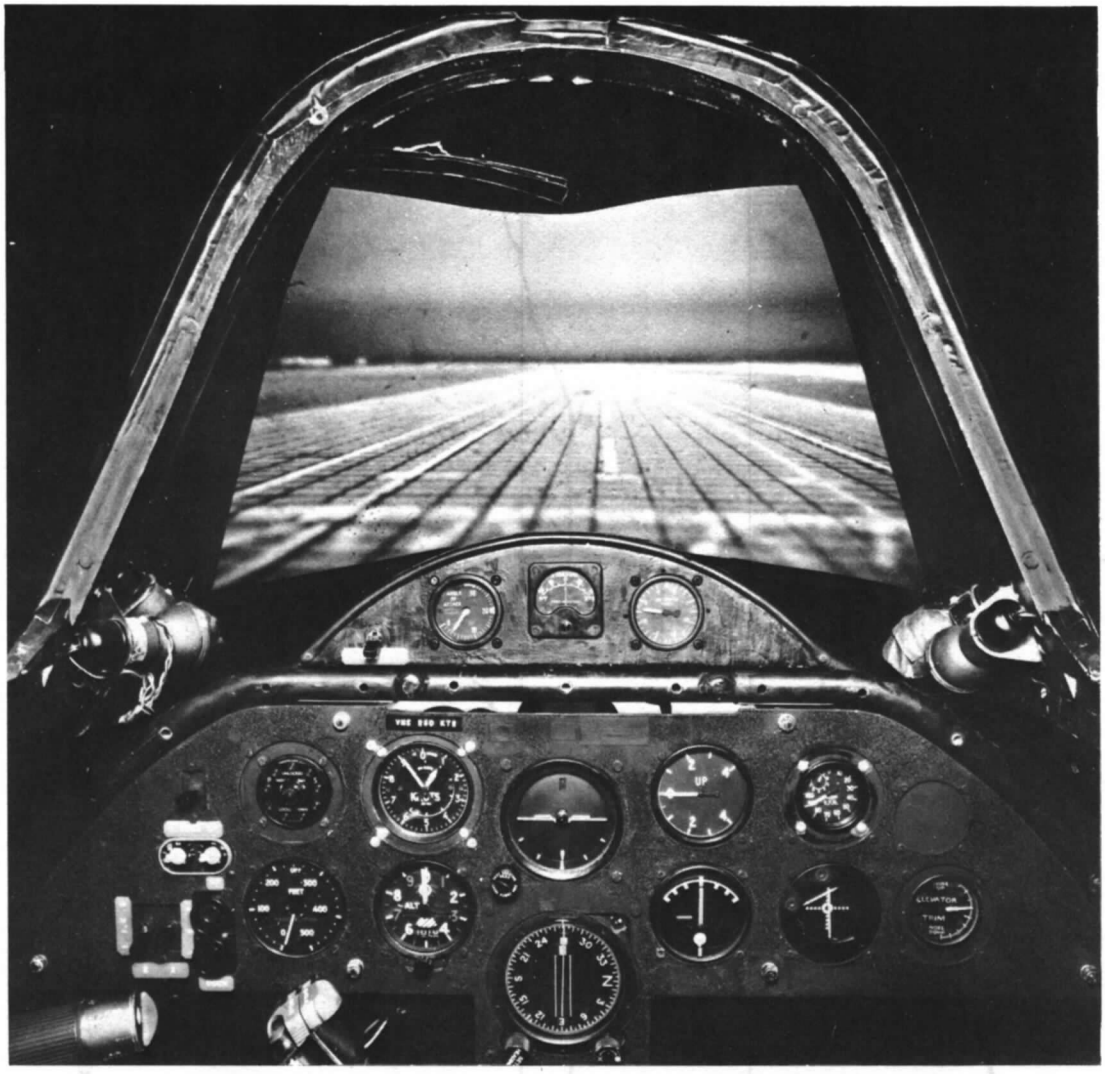

FIG. 4. Simulator instrument panel and visual display.

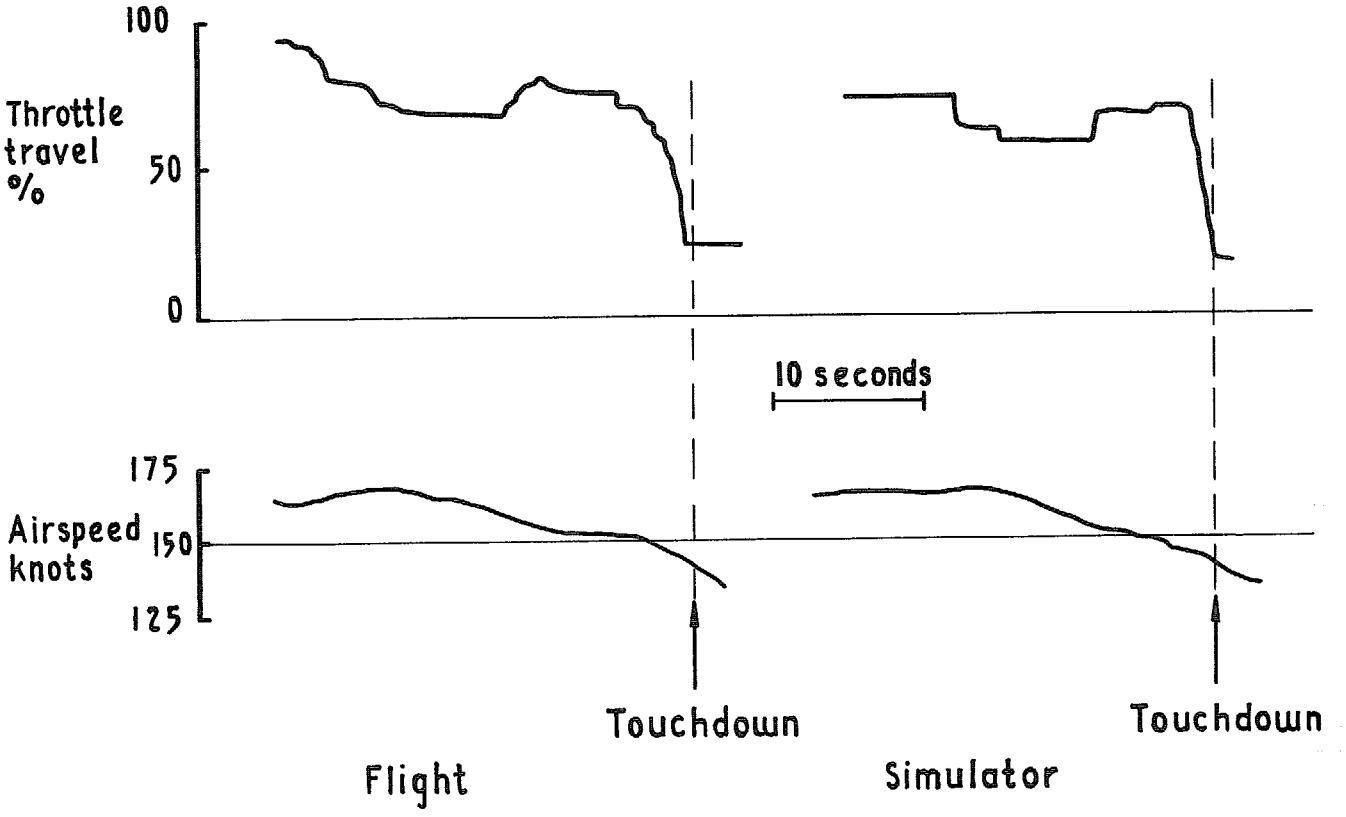

FIG. 5. Throttle usage during approaches in flight and simulator.

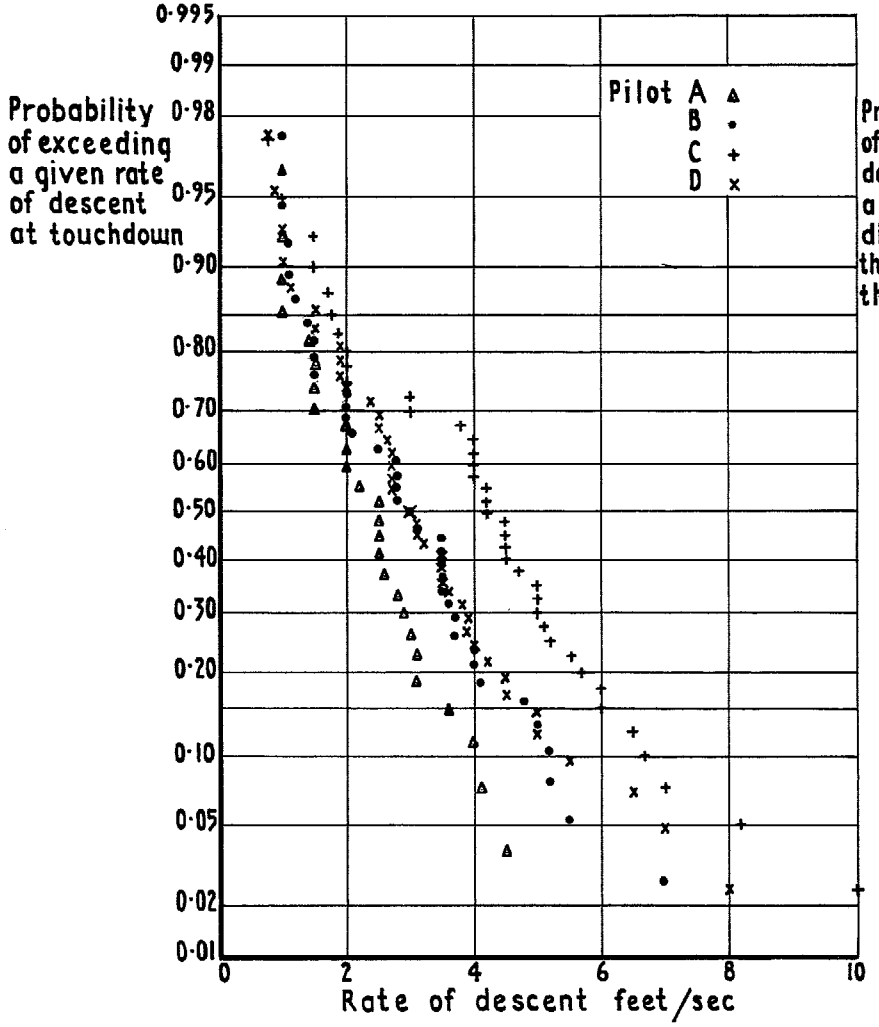

A Rate of descent at touchdown.

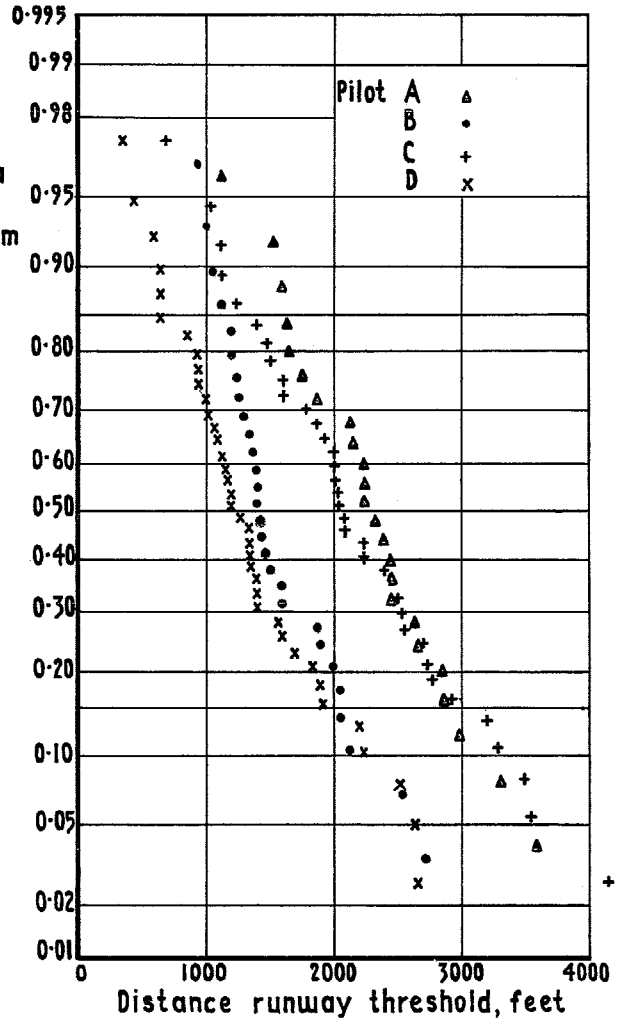

B Touchdown distance.

FIG. 6a & b. Cumulative probability plots of touchdown rate of descent and distance.

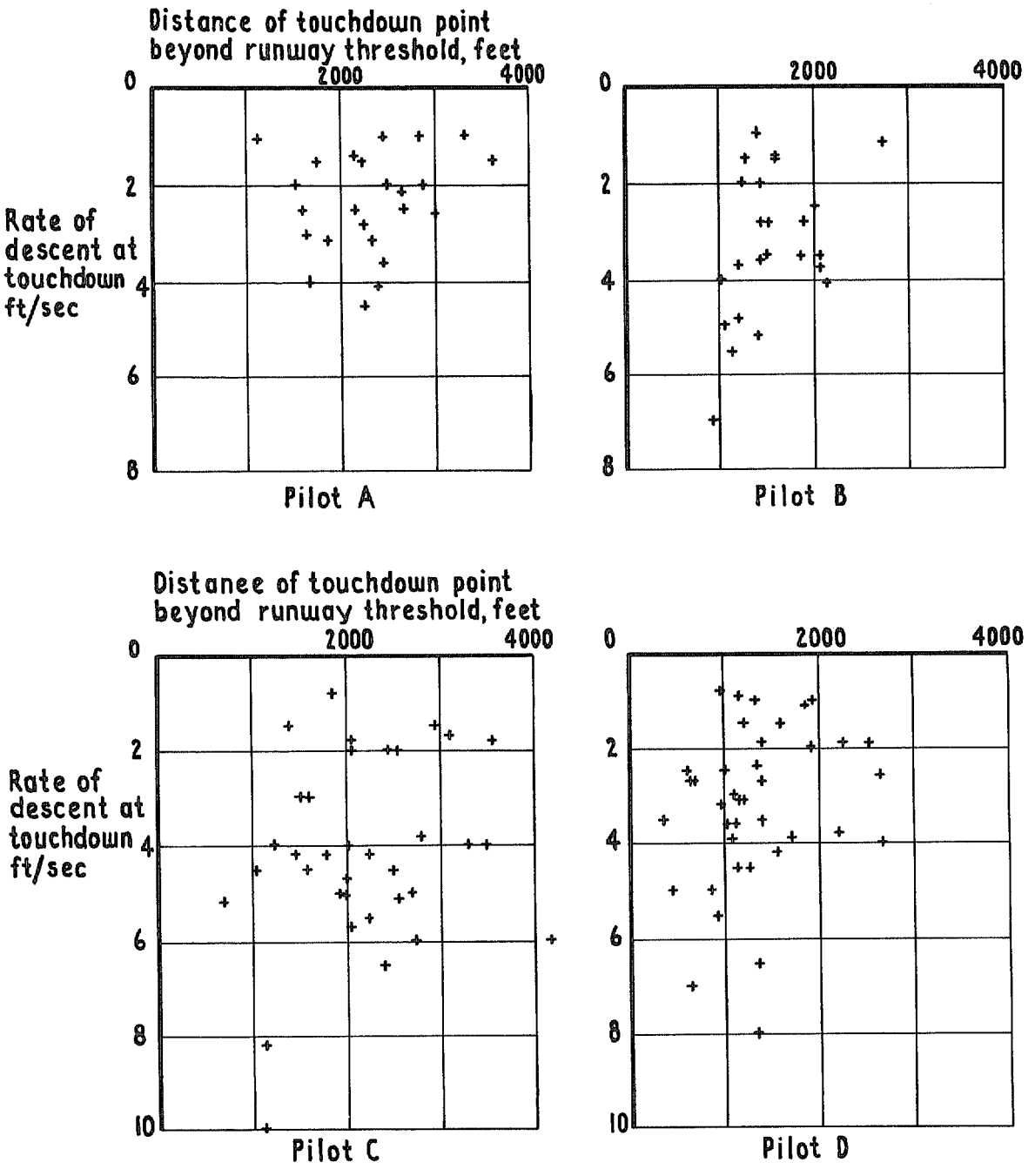

FIG. 7. Plots of touchdown point and rate of descent.

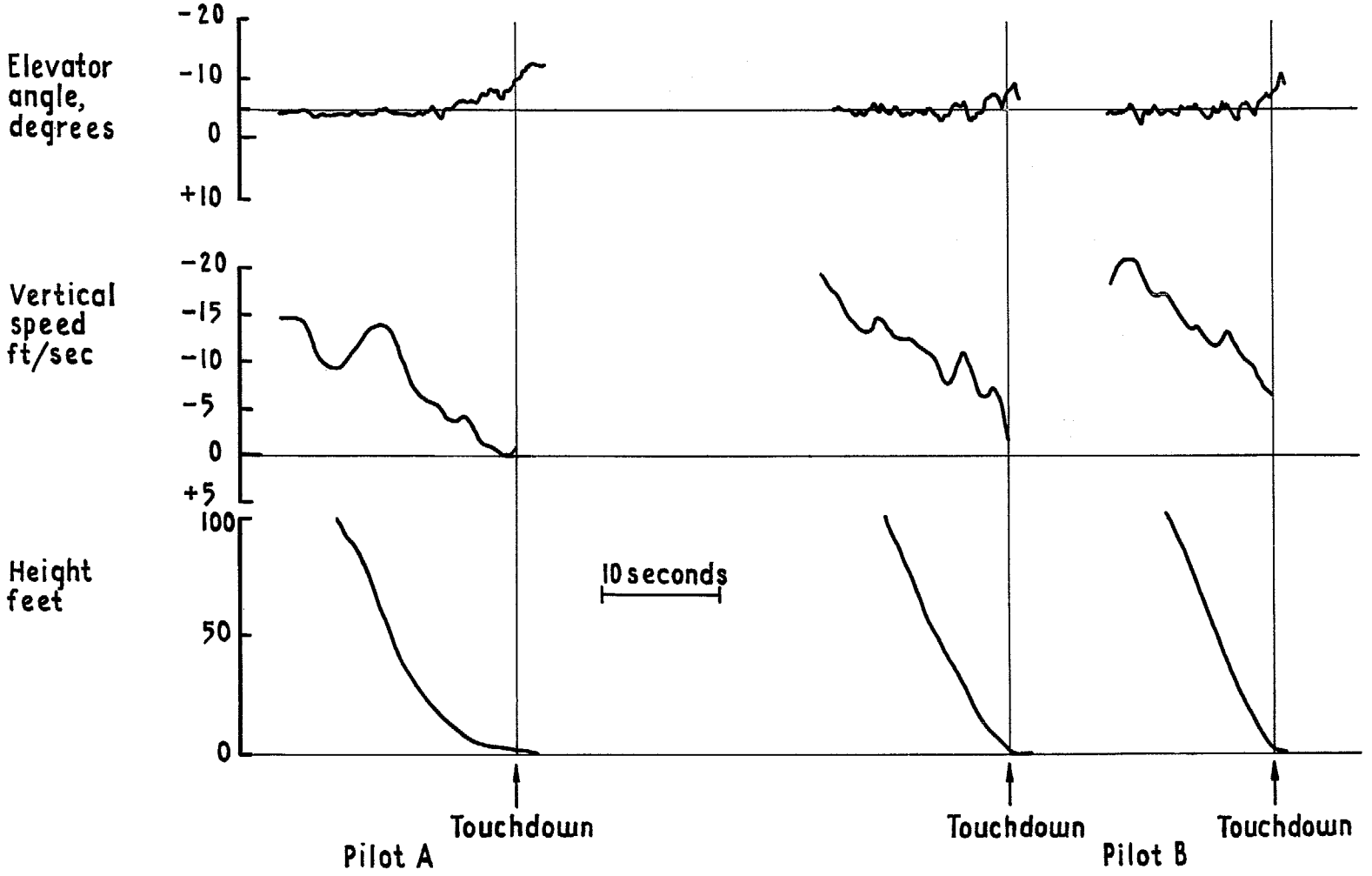

FIG. 8. Flare technique.

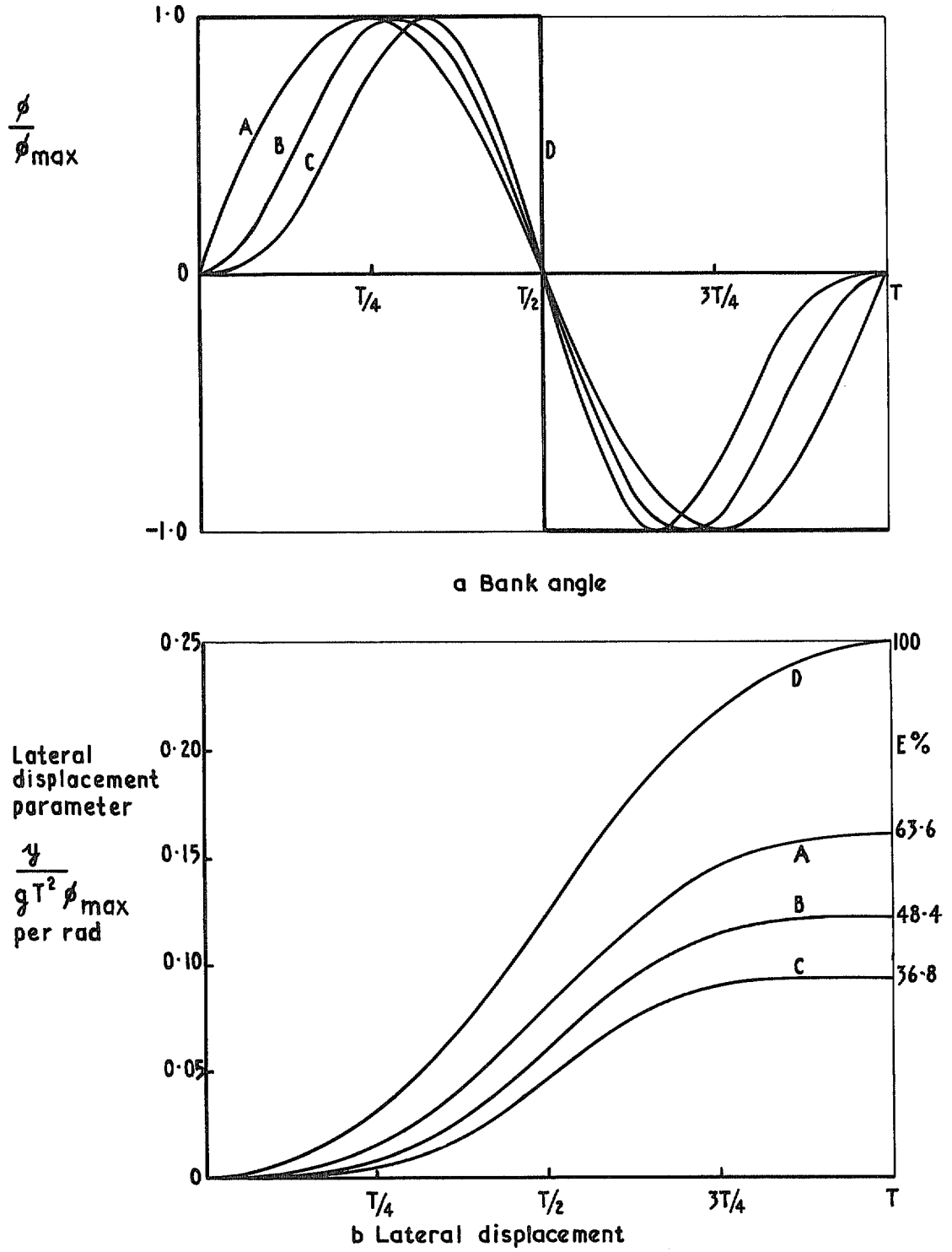

FIG. 9a & b. Bank angle and lateral displacement time-histories of reference 12.

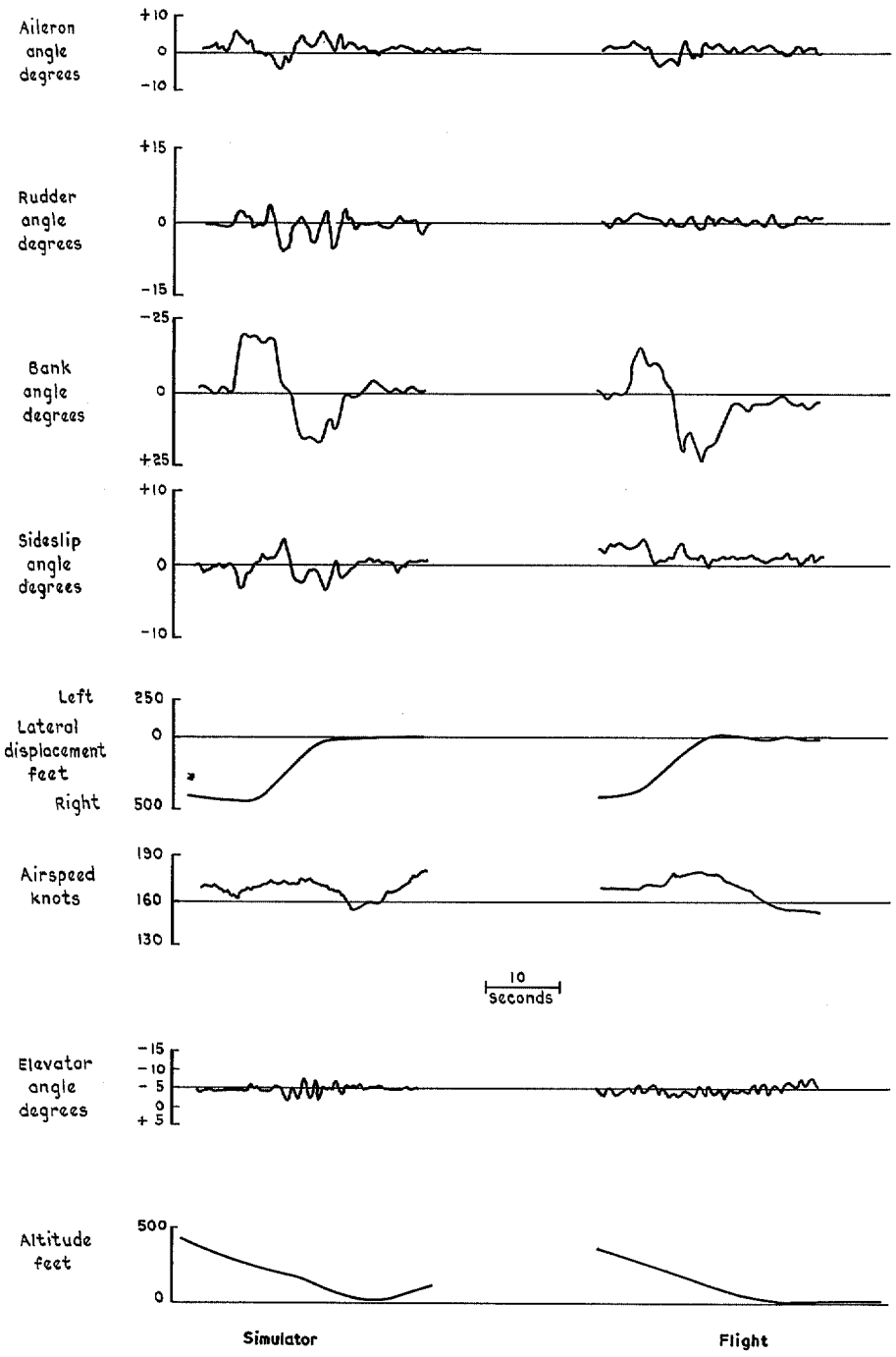

FIG. 10. Time histories of sidestep manoeuvres in simulator and in flight.

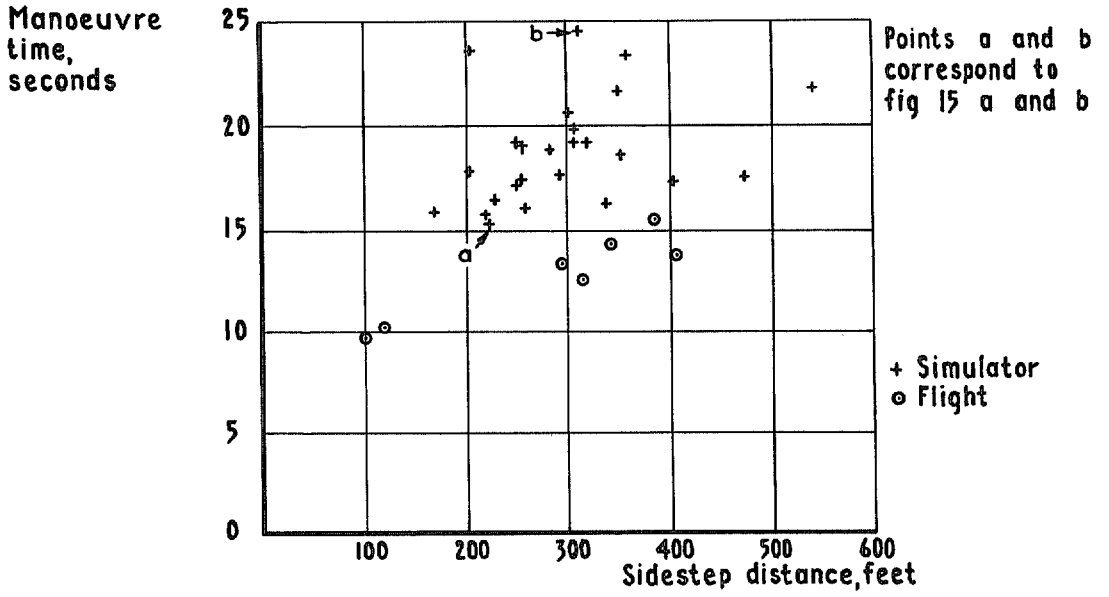

FIG. 11. Manoeuvre time v sidestep distance.

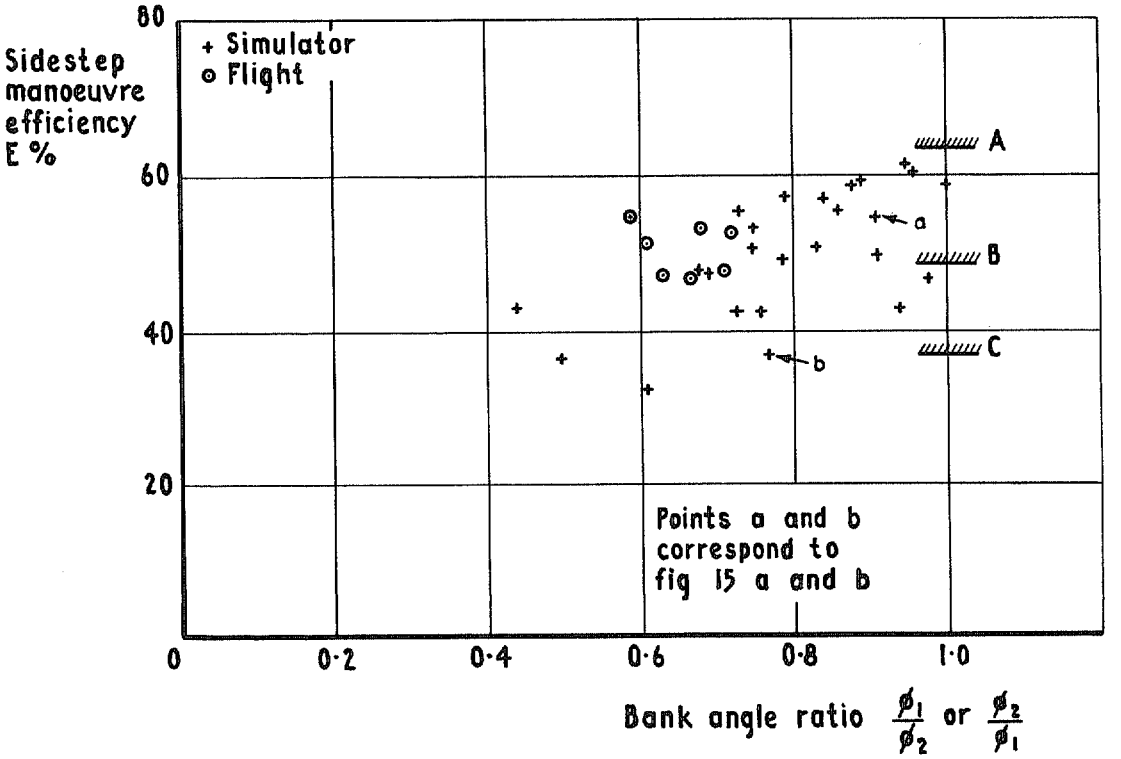

FIG. 12. Sidestep manoeuvre efficiency v bank angle ratio.

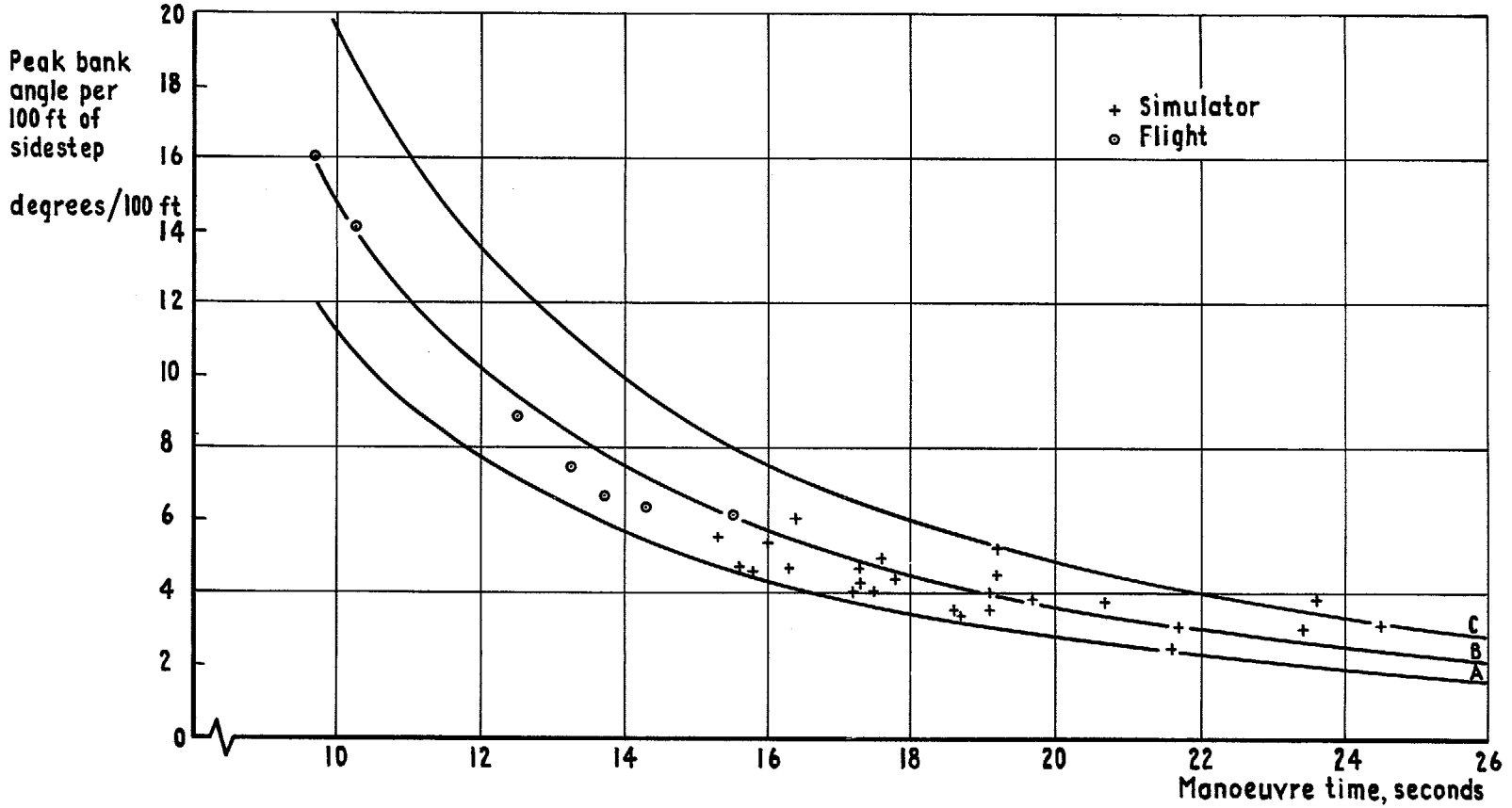

FIG. 13. Peak bank angle v sidestep manoeuvre time.

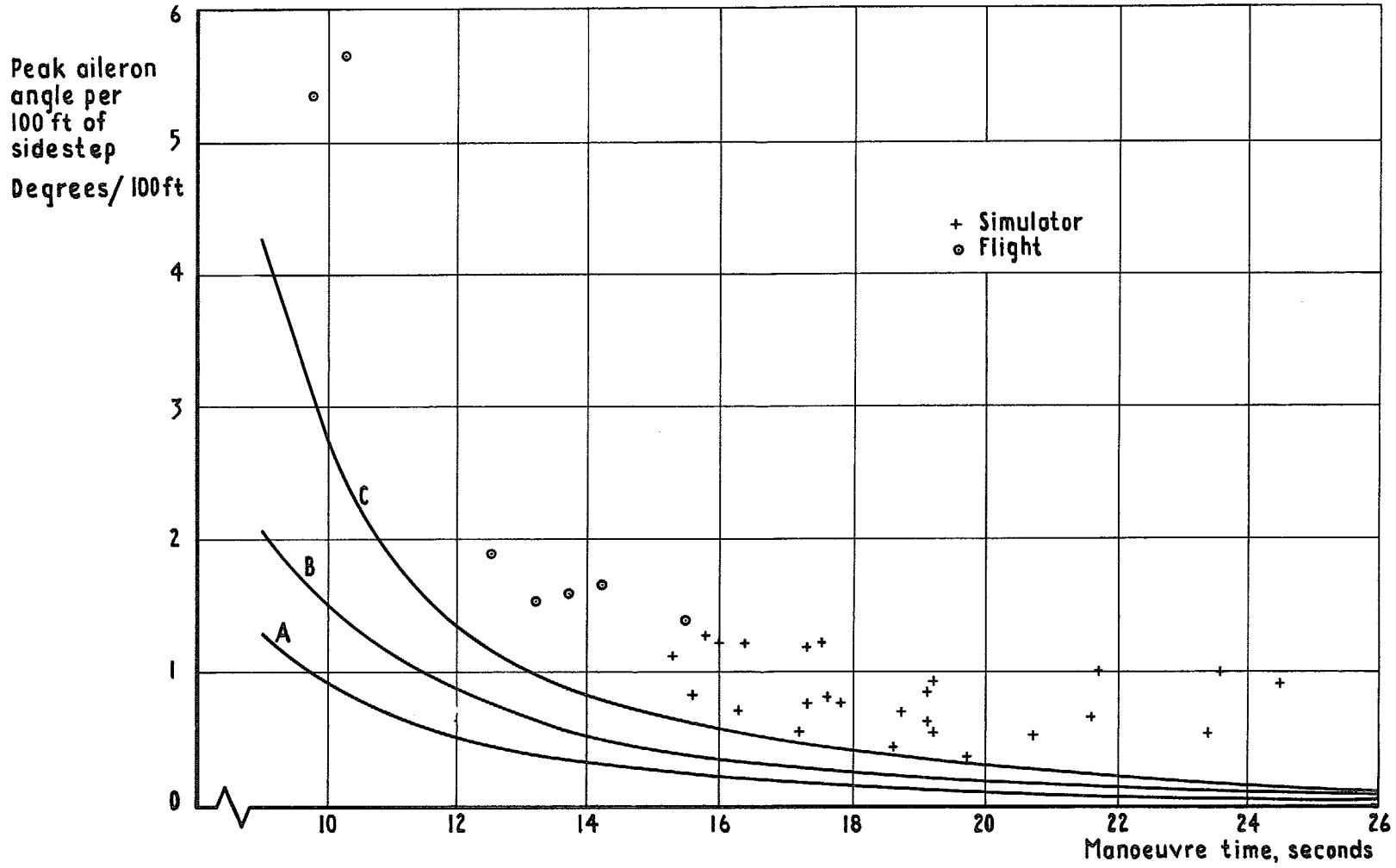

FIG. 14. Peak aileron angle v sidestep manoeuvre time.

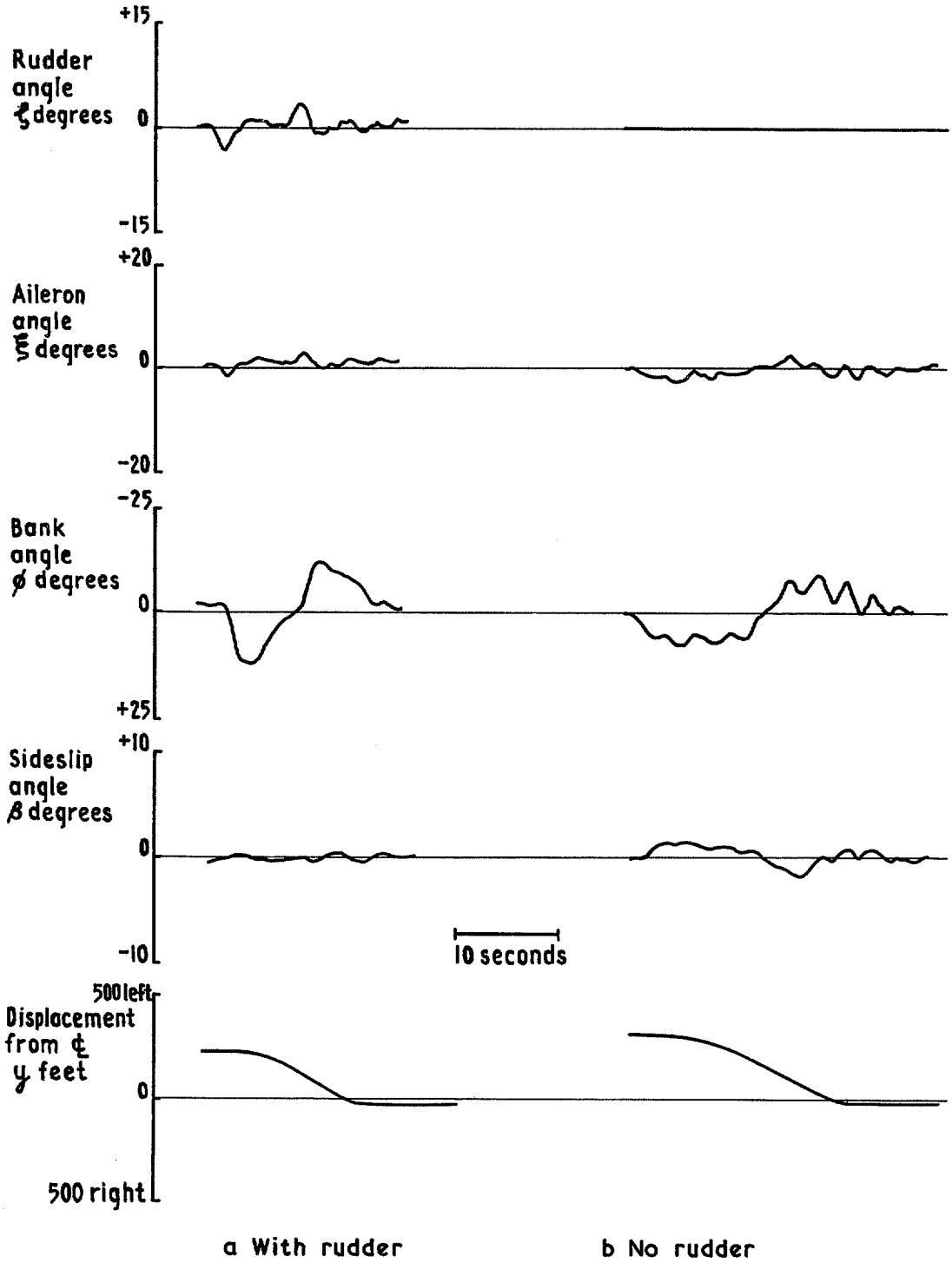

FIG. 15a & b. Sidestep manoeuvres with and without the use of rudder.

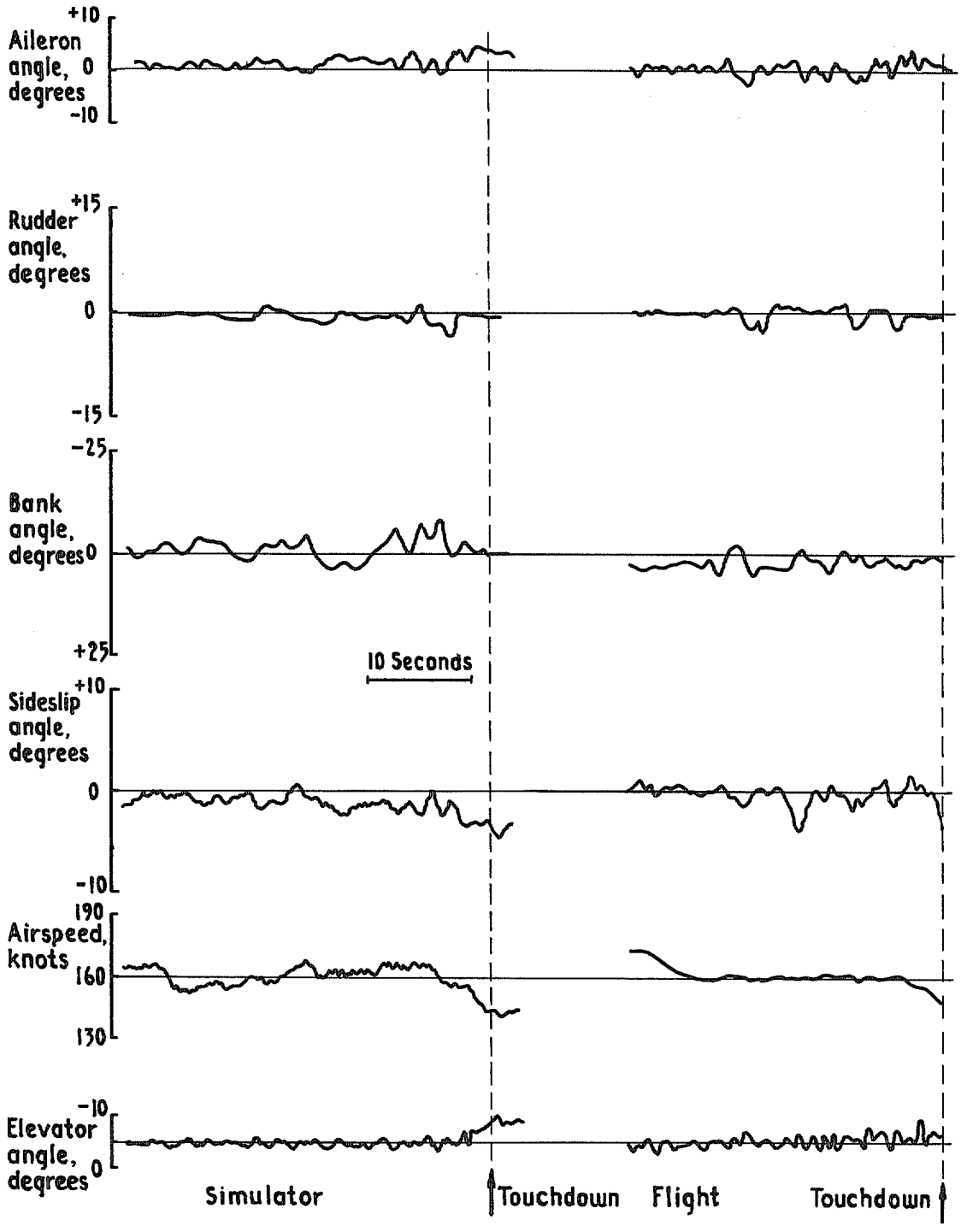

FIG. 16. Time histories of approaches in 12 knot crosswinds, simulator and flight.

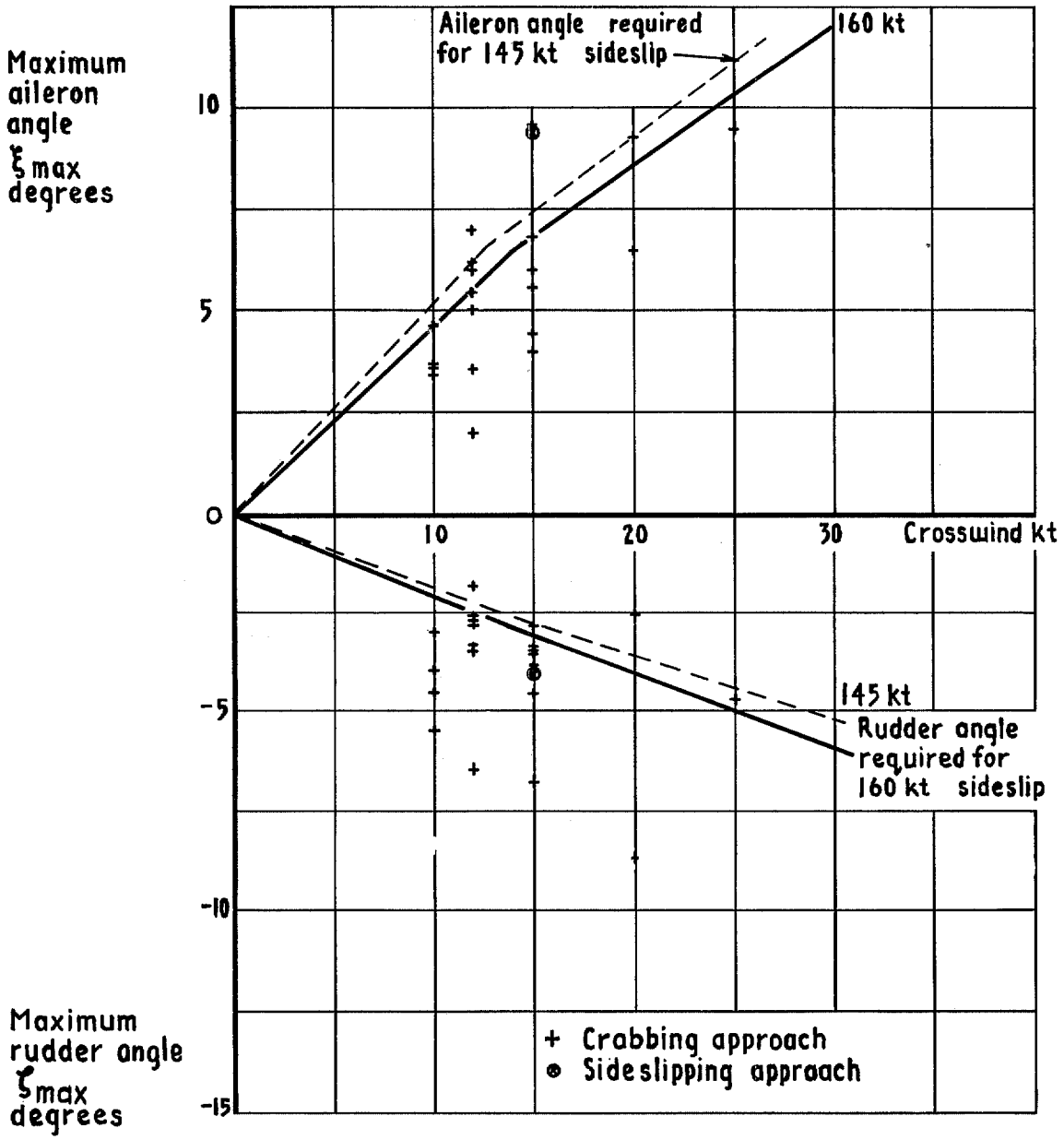

FIG. 17. Maximum control usage during crosswind landings.

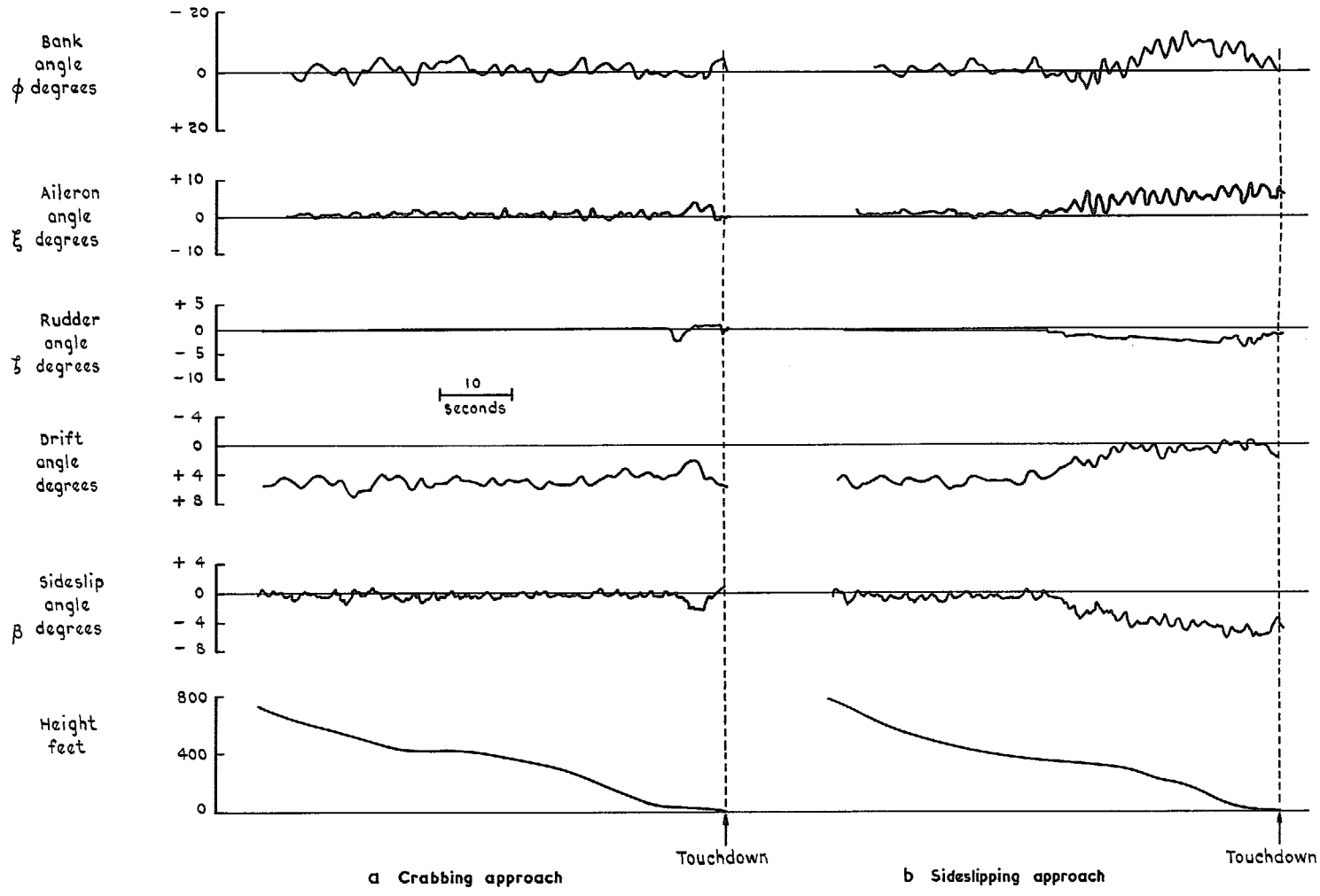

FIG. 18a & b. Crosswind approach techniques (15kt crosswind).

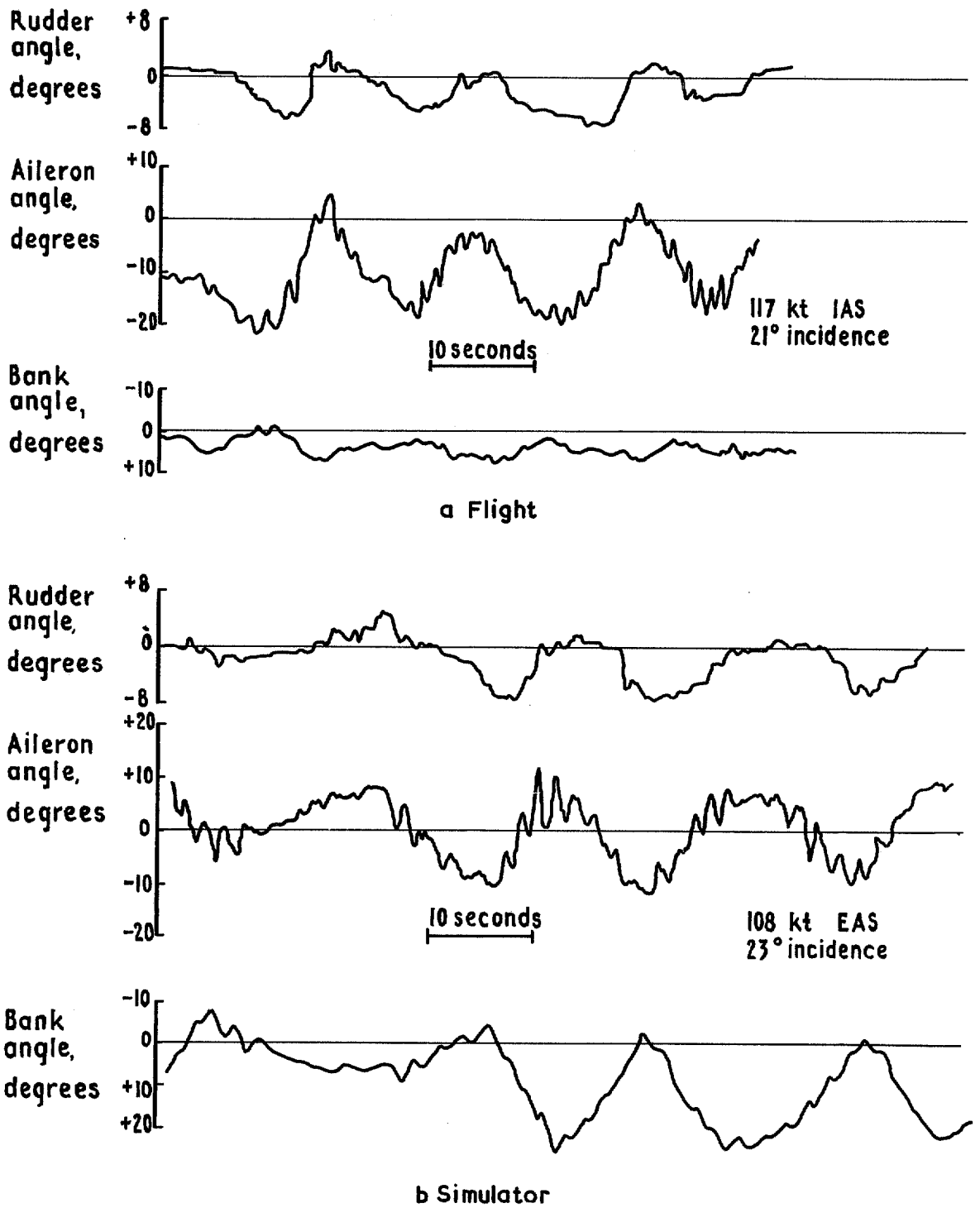

FIG. 19a & b. Lateral control difficulty at high incidence.

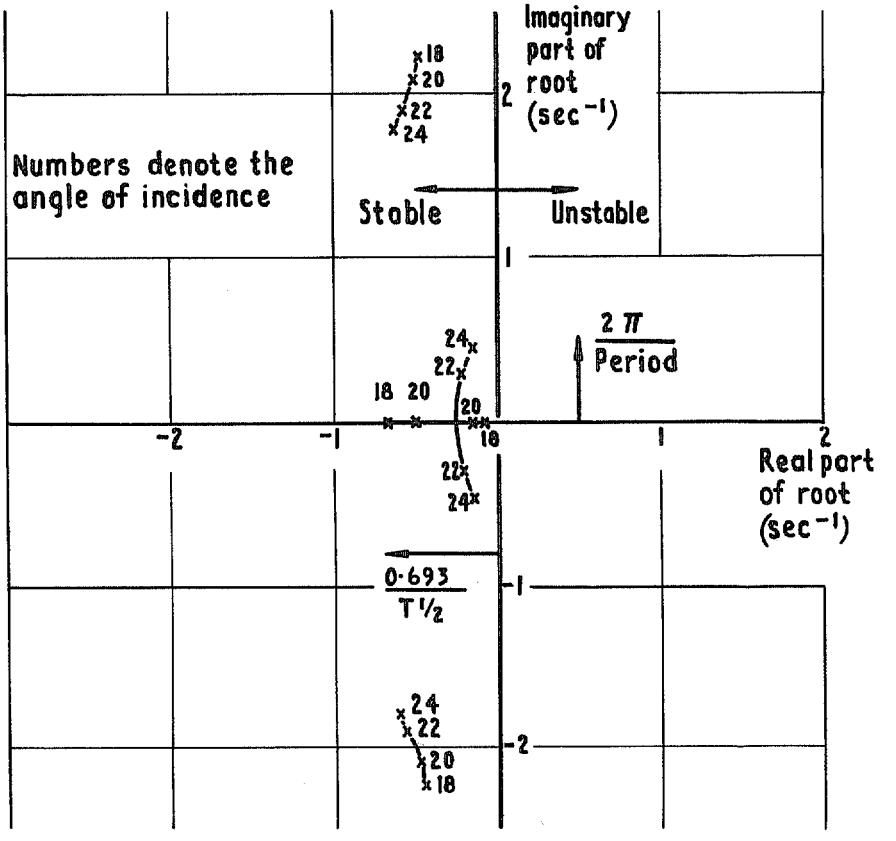

a Stability roots of unconstrained aircraft

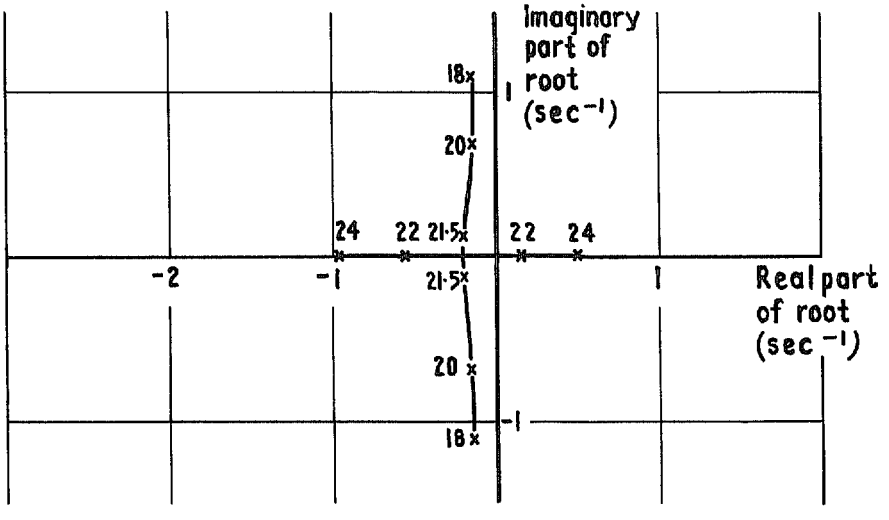

b Stability roots when bank angle is perfectly constrained by ailerons

FIG. 20a & b. Lateral stability roots.

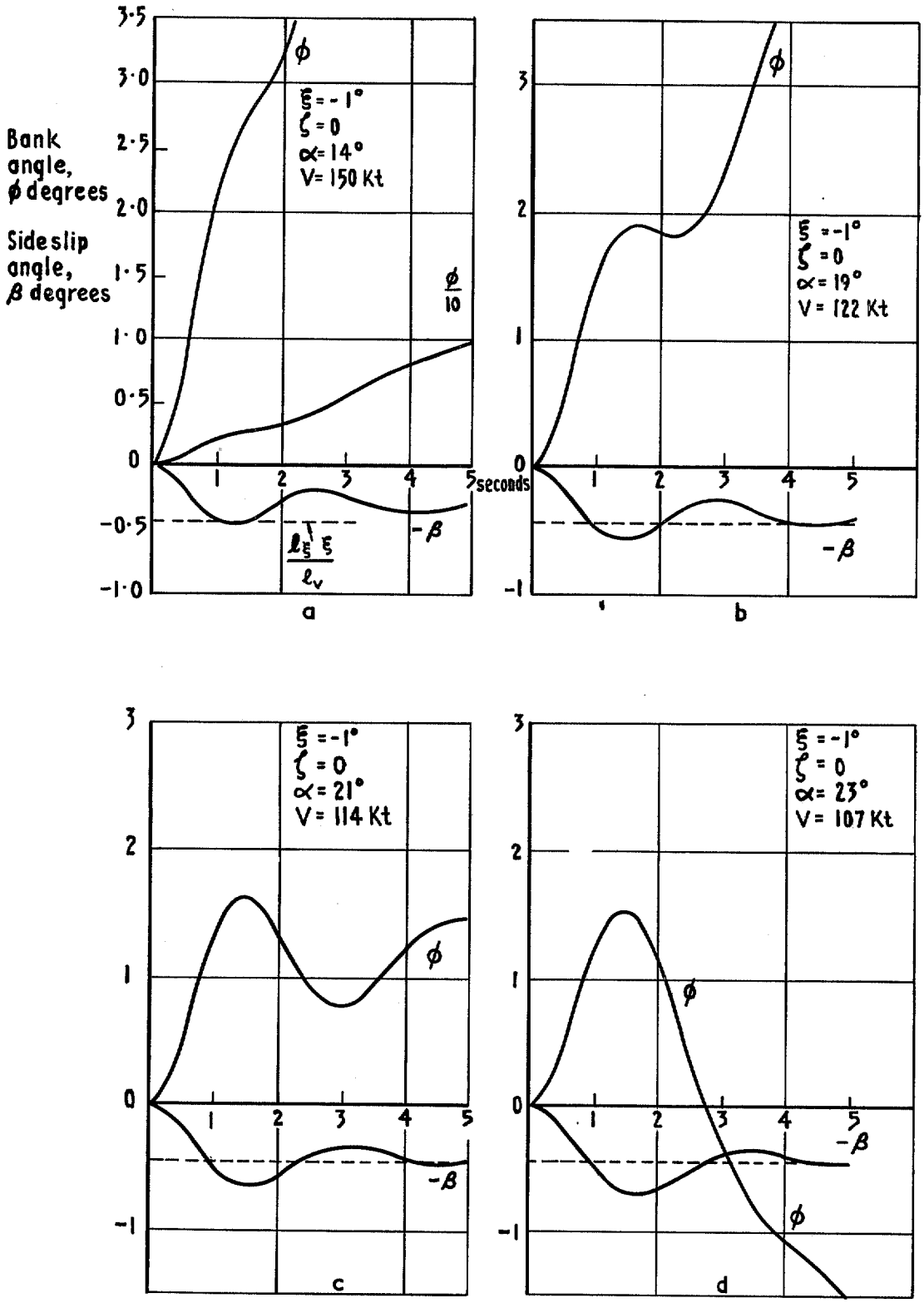

FIG. 21a–d. Response to step input of aileron and rudder.

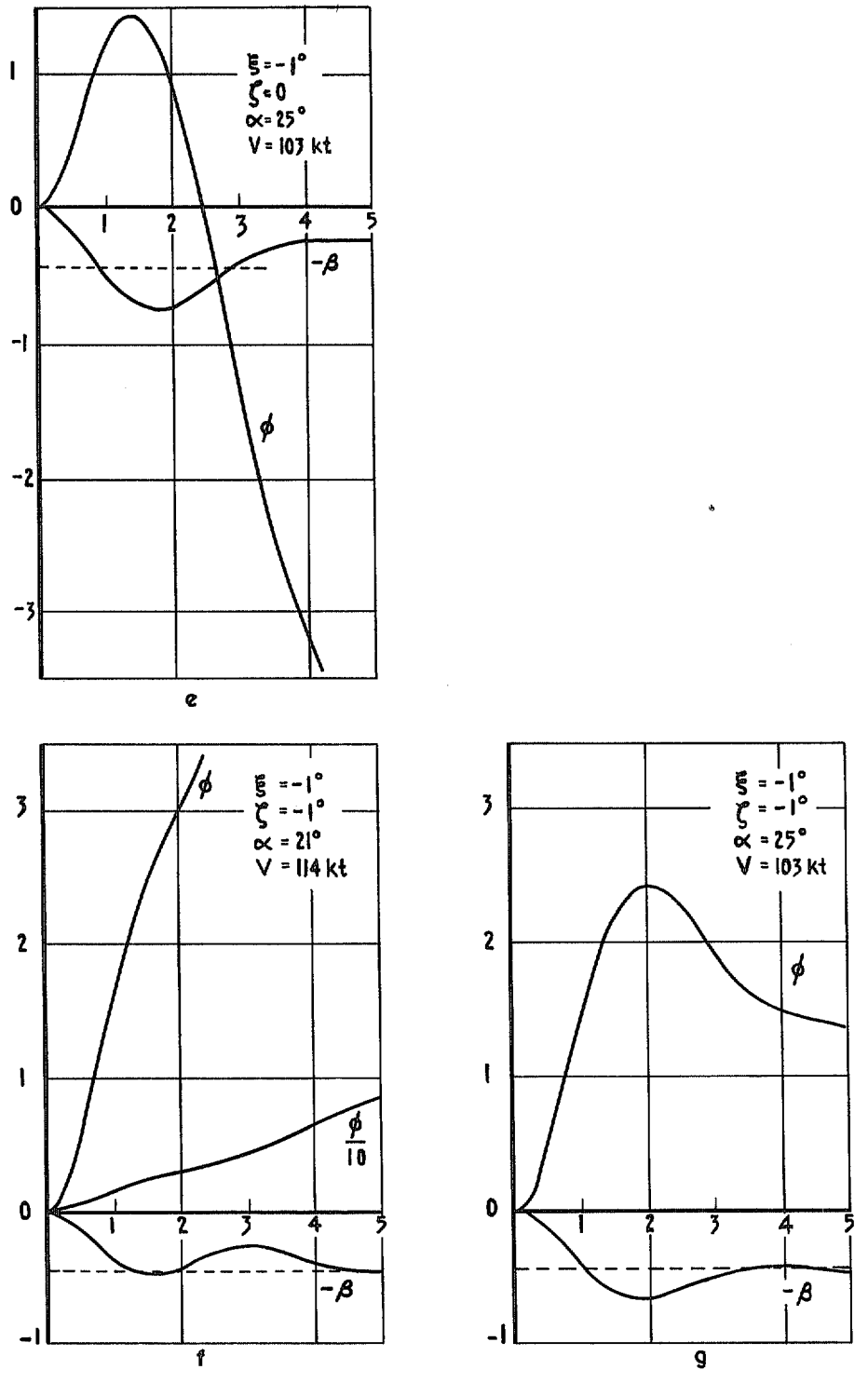

FIG. 21e–g. Response to step input of aileron and rudder.

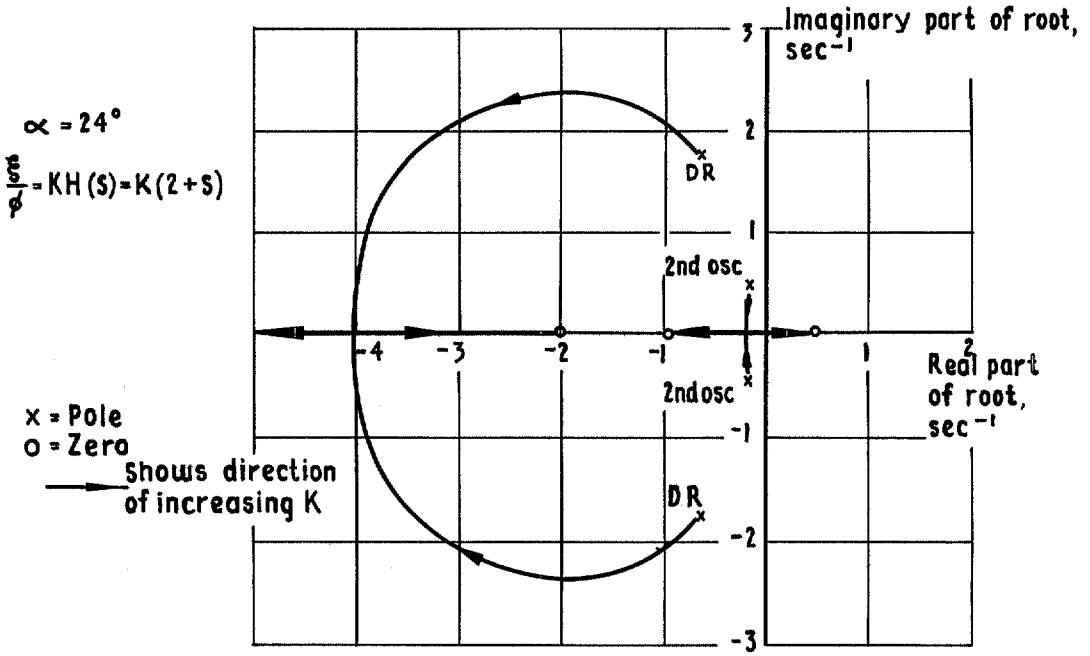

a Aileron alone

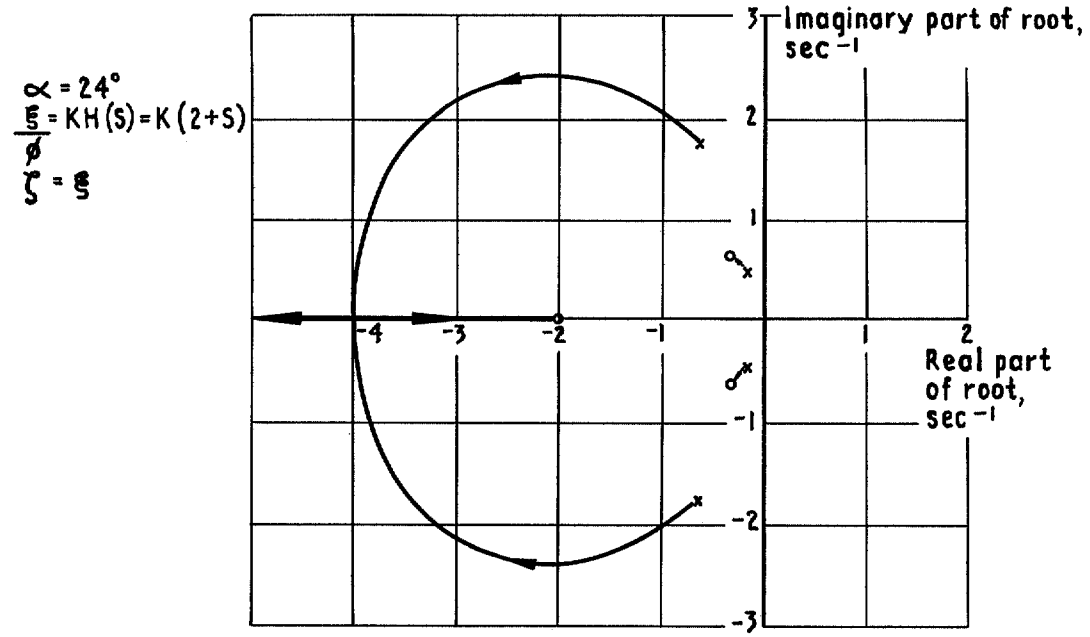

b Aileron and rudder

FIG. 22a & b. Root locus plots for aileron and aileron-with-rudder control of bank angle.

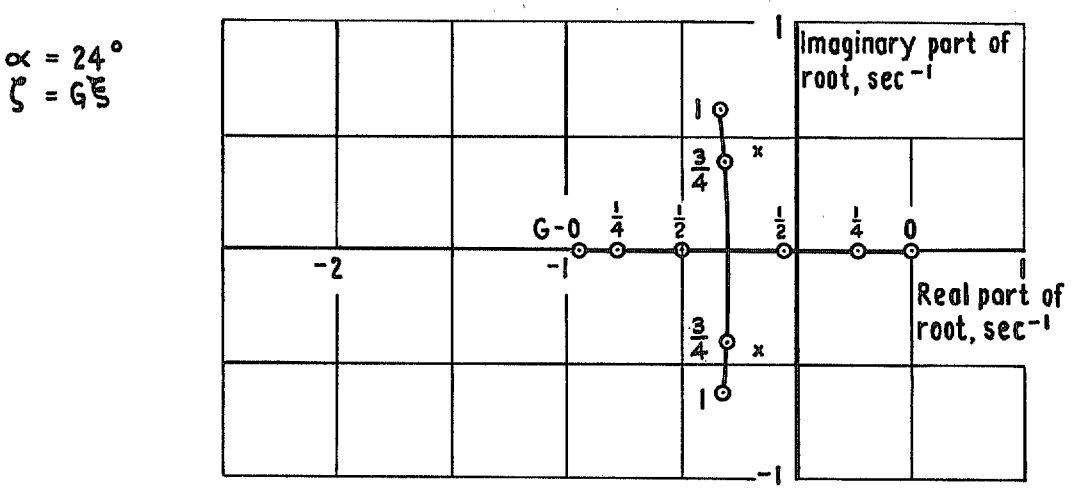

FIG. 23. Loci of the zeros of the aircraft transfer function as a function of aileron-rudder gearing.

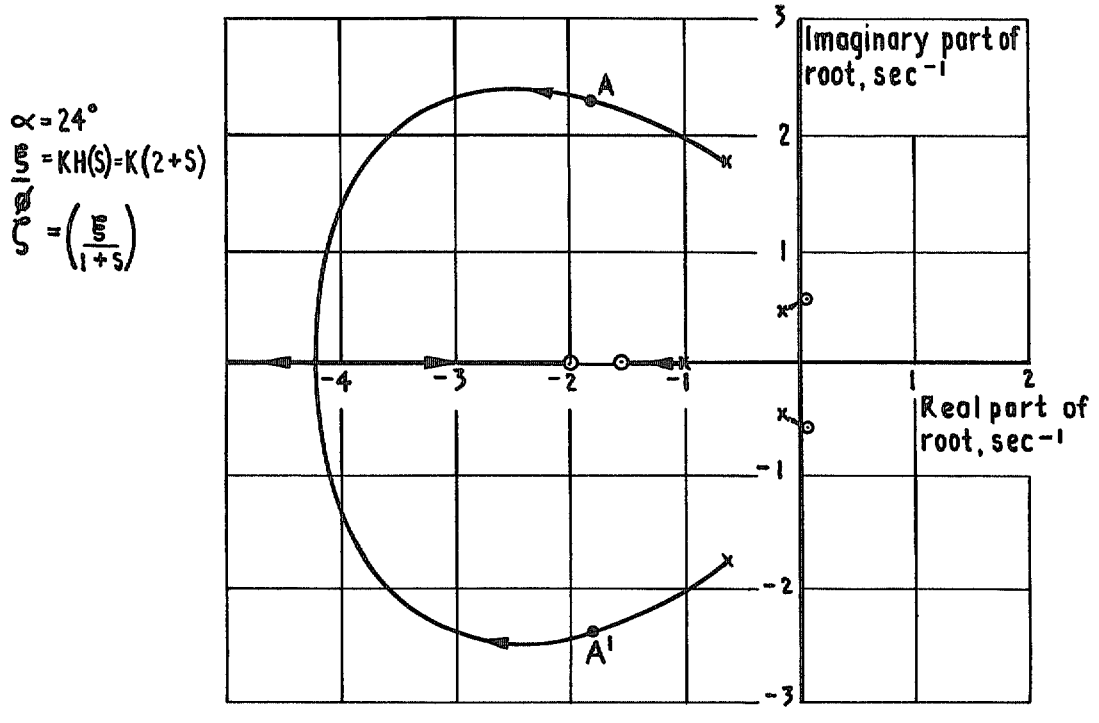

FIG. 24. Root locus plot for aileron-with-rudder control of bank angle, rudder lagging aileron by 1 second.

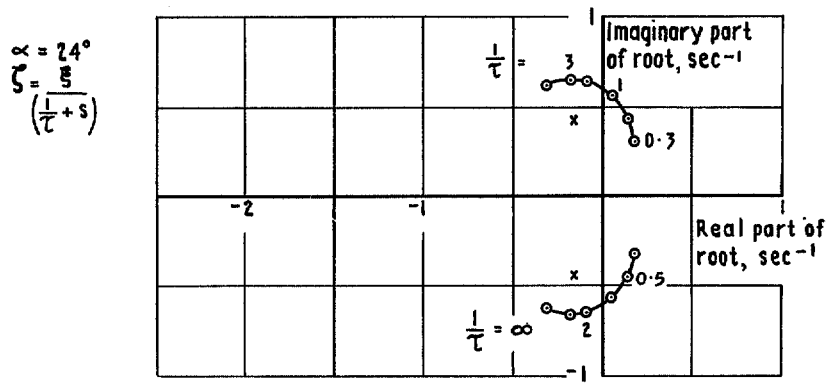

FIG. 25. Loci of the complex zeros of the aircraft transfer function as a function or rudder to aileron lag.

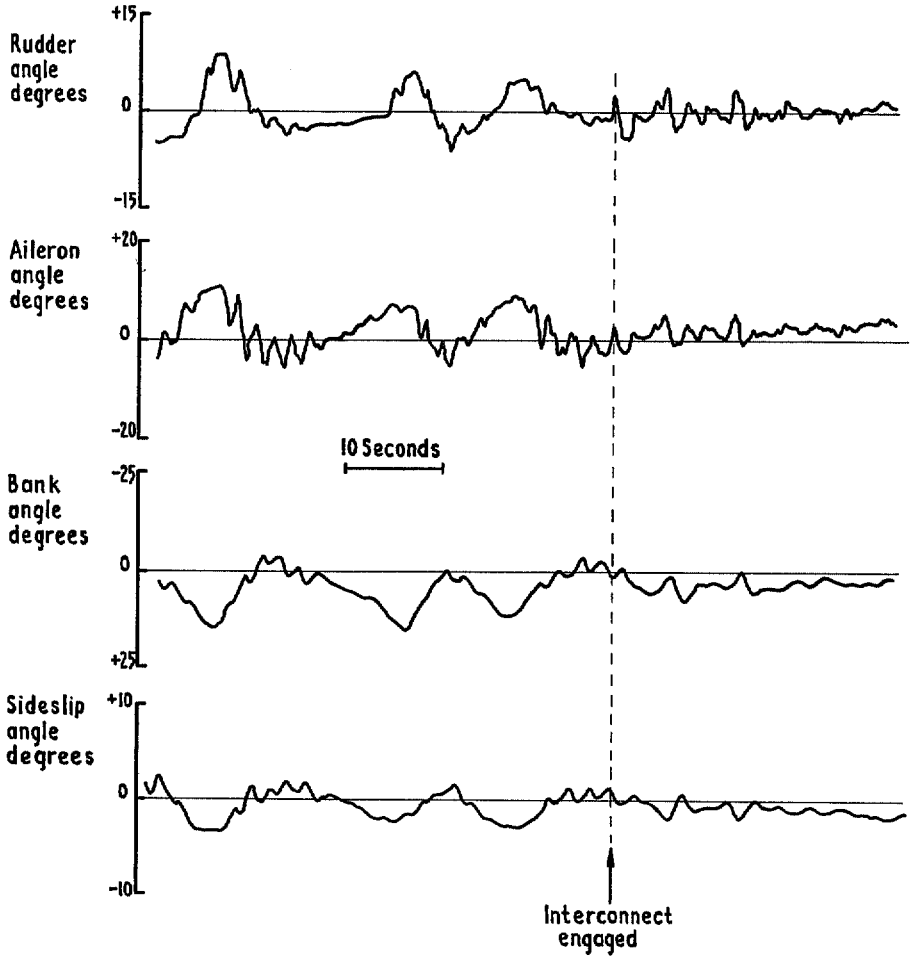

FIG. 26. Lateral control at high incidence in simulator with and without rudder interconnect.

Printed in Wales by Offset Litho for Her Majesty's Stationery Office by Allens Printers (Wales) Limited.
Dd. 502110 K.5.

Published by
HER MAJESTY'S STATIONERY OFFICE

To be purchased from
49 High Holborn, London WC1V 6HB
13a Castle Street, Edinburgh EH2 3AR
109 St Mary Street, Cardiff CF1 1JW
Brazennose Street, Manchester M60 8AS
50 Fairfax Street, Bristol BS1 3DE
258 Broad Street, Birmingham B1 2HE
80 Chichester Street, Belfast BT1 4JY
or through booksellers

SBN 11 470410 4